

Supporting Information for
Phosphine-Phenoxy Nickel Catalysts for Ethylene/Acrylate
Copolymerization: Olefin Coordination and Complex Isomerisation Studies
Relevant to the Mechanism of Catalysis

Manar M. Shoshani[†], Shuoyan Xiong[†], James J. Lawniczak, Xinglong Zhang, Thomas F. Miller III*, and Theodor Agapie*

*To whom correspondence should be addressed, E-mail: agapie@caltech.edu.

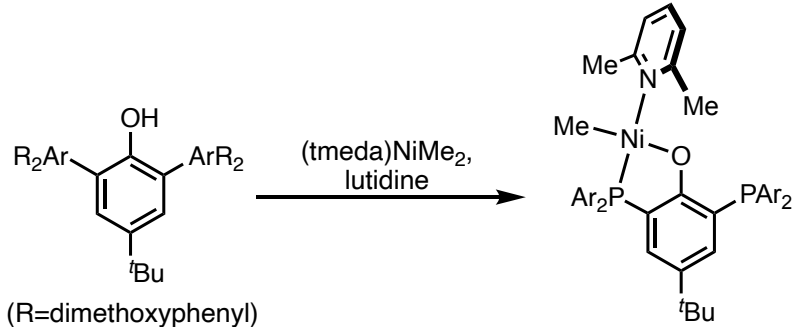
Division of Chemistry and Chemical Engineering, California Institute of Technology, 1200 East California Boulevard MC 127-72, Pasadena, California 91125, United States

1. General considerations	S2
2. Synthesis of transition metal complexes	S3
3. NMR characterization	S17
4. Quantitative determination of ligand binding strengths	S46
5. Supplemental information for olefin polymerization	S53
6. Crystallographic information	S60
7. Computational details	S65
8. References	S67

1. General Considerations

All air- and water-sensitive compounds were manipulated under N₂ or Ar using standard Schlenk or glovebox techniques. The solvents for air- and moisture-sensitive reactions were dried over sodium benzophenone ketyl or calcium hydride or by the method of Grubbs.¹ Deuterated solvents were purchased from Cambridge Isotopes Lab, Inc.; C₆D₆, and C₇D₈ was dried over a purple suspension with Na/benzophenone ketyl and vacuum transferred. Ethylene (99.999%) was purchased from Matheson Tri-Gas and used without further purification. 2,6-lutidine was dried with sieves and distilled over AlCl₃ to remove 3-picoline and 4-picolline. 4-CF₃ pyridine, pentafluoropyridine, 2-picoline, and 4-tert-butyl pyridine were dried by stirring over CaH₂ for greater than 12 hours and distilling. PEt₃ was purchased from Sigma Aldrich and purified by distillation prior to use. Triethylphosphine oxide was purchased from Combiblocks and used without further purification. 1-hexene was purchases from Sigma-Aldrich and distilled over Å sieves. t-butyl acrylate was dried over 3 Å sieves for greater than 72h, vacuum transferred, and passed over an activated alumina plug. Ligand **POPH**, **PONapH**, complexes **1**, **2**, **2lut-Me**, **2-CCO**,² NiMe₂TMEDA,³ and Nipy₂(CH₂Si(CH₃)₃)⁴ were synthesized according to literature procedures. All ¹H, ¹³C, and ³¹P spectra of organic and organometallic compounds were recorded on Varian INOVA-400, or 500, or Bruker Cryoprobe 400 spectrometers. ¹H and ¹³C chemical shifts are reported relative to residual solvent resonances.

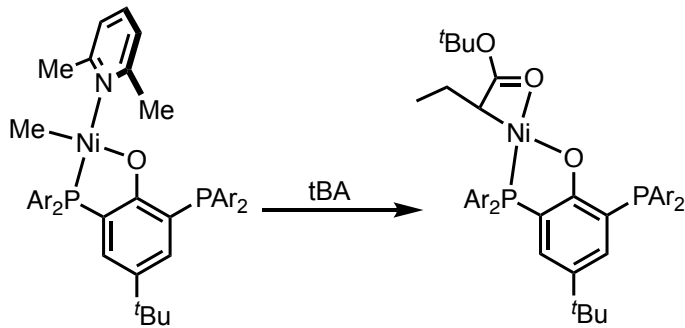
2. Synthesis of Transition Metal Complexes:



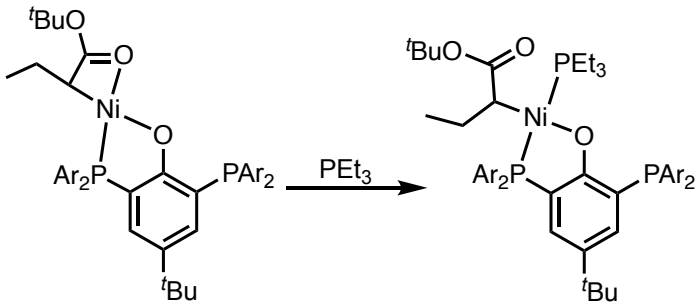
1lut-Me: In the glove box, to a thawing solution of NiMe₂(TMEDA) (38 mg, 0.19 mmol) in toluene (2 mL) was added a thawing solution of **POPH** (144 mg, 0.19 mmol) and 40 equivalents of 2,6-lutidine (717 mg, 7.54 mmol) in toluene (2 mL). The yellow solution was stirred while warming to room temperature for 30 minutes. After stirring for additional 30 min, all volatiles were removed from solution which was triturated with n-pentane (3 x 5 mL). The resulting residue was washed by n-pentane (5 mL) and diethyl ether (5 mL). The solids were collected via a filtration yielding spectroscopically pure **1lut-Me** (62 mg, 35 % Yield).

¹H NMR (400 MHz, C₆D₆): δ 7.58-7.52 (m, 1H, ArH), 7.14-7.05 (m, 5H, ArH), 6.75 (t, ³J_{HH} = 7.6 Hz, 1H, lutidine-ArH), 6.40 (d, ³J_{HH} = 7.6 Hz, 1H, lutidine-ArH), 6.36 (dd, ³J_{HH} = 8.2 Hz, ⁴J_{HP} = 3.4 Hz, 4H, ArH), 6.33 (dd, ³J_{HH} = 8.2 Hz, ⁴J_{HP} = 3.4 Hz, 4H, ArH), 3.37 (s, 6H, lutidine-CH₃), 3.30 (s, 12H, -OCH₃), 3.20 (s, 12H, -OCH₃), 1.22 (s, 9H, -C(CH₃)₃), -0.77 (d, J = 6.4 Hz, 3H, -NiCH₃). ¹³C{¹H} NMR (101 MHz, C₆D₆): δ 163.56 (d, J_{CP} = 8.3 Hz, 4C, Aryl-C), 161.32 (s, 4C, Aryl-C), 159.24 (s, 2C, Aryl-C), 134.98 (s, 1C, Aryl-C), 132.43 (d, J_{CP} = 2.8 Hz, 1C, Aryl-C), 131.26 (s, 1C, Aryl-C), 129.42 (s, 2C, Aryl-C), 128.97 (s, 1C, Aryl-C), 128.23 (d, 2C, Aryl-C), 128.20 (s, 1C, Aryl-C), 125.15 (d, J_{CP} = 36.8 Hz, 1C, Aryl-

C), 124.97 (s, 1C, Aryl-C), 120.46 (s, 2C, Aryl-C), 118.89 (d, $J_{CP} = 31.3$ Hz, 1C, Aryl-C), 113.02 (d, $J_{CP} = 44.8$ Hz, 1C, Aryl-C), 105.26 (s, 4C, Aryl-C), 104.25 (s, 4C, Aryl-C), 55.69 (s, 2C, Aryl-C), 55.67 (s, 2C, Aryl-C), 55.02 (s, 4C, Aryl-C), 33.78 (s, 1C, -C(CH₃)₃), 32.05 (s, 3C, -C(CH₃)₃), 25.71 (s, 2C, -CH₃), -23.85 (d, $J=35.1$ Hz, -NiCH₃). ³¹P{¹H} NMR (121 MHz, C₆D₆, 298 K): δ - 5.08 (d, $J_{PP} = 11.0$ Hz, 1P), - 52.71 (d, $J_{PP} = 11.0$ Hz, 1P). Anal. Calcd(%) for C₅₀H₅₉NNiO₉P₂: C: 63.98, H: 6.34, N: 1.49; found: C: 67.51, H: 6.02, N: 1.38.

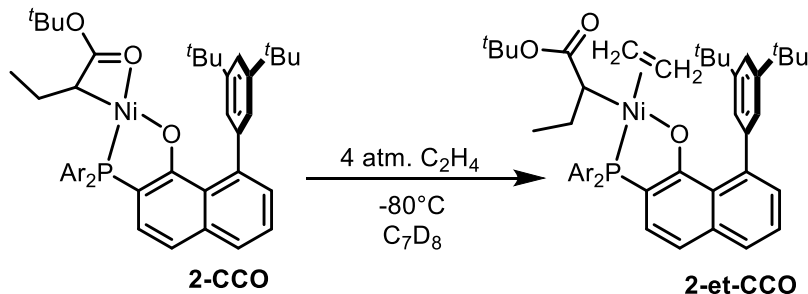


1-CCO: In the glove box, to a stirring solution of **1lut-Me** (73.1 mg, 0.078 mmol) in toluene (2 mL) was added 5 equiv. of tert-butyl acrylate (49.9 mg, 0.39 mmol). After 1 h, all volatiles were removed from the solution and the residue was triturated with cold hexanes (3*5 mL). The remaining residue was then washed with cold hexanes (5 mL) to afford **1-CCO** as reddish solids (28 mg, 38% yield). Complex **1-CCO** was only characterized by ¹H and ³¹P{¹H} NMR due to its low thermal stability. ¹H NMR (400 MHz, C₆D₆): δ 7.35 (d, $^3J_{HP} = 12.7$ Hz m, 1H, ArH), 7.07-6.81 (overlapping m, 5H, ArH), 6.38 (d, $^3J_{HH} = 8.2$ Hz, 4H, ArH), 6.16 (d, $^3J_{HH} = 8.2$ Hz, 4H, ArH), 3.33 (broad s, 12H, -OCH₃), 3.26 (broad s, 12H, -OCH₃), 1.56 (s, 9H, -OC(CH₃)₃), 1.34 (m, 1H, Ni-alkyl), 1.11 (overlapping m, 10H, -C(CH₃)₃ + Ni-alkyl), 0.86 (overlapping m, 4H, Ni-alkyl). ³¹P{¹H} NMR (121 MHz, C₆D₆, 298 K): δ ~ 4.5 (broad), ~ 8.0 (broad), - ~51 (broad, 1P).



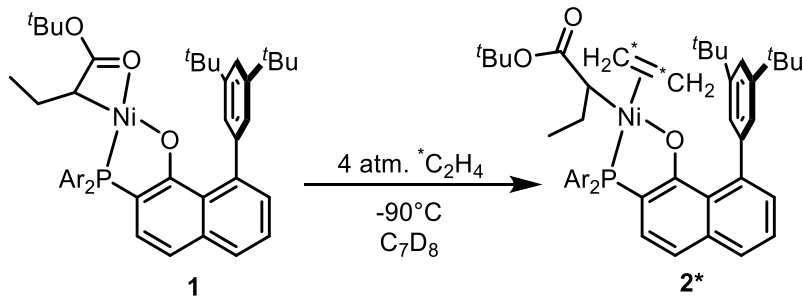
1P-CCO: In the glove box, to a solution of **1-CCO** (19.2 mg, 0.02 mmol) in toluene (2 mL) was added 5 equiv. of triethylphosphine (11.8 mg, 0.10 mmol). After stirred for 15 min, all volatiles were removed under vacuum, affording quantitative formation of **1P-CCO** (21.2 mg, >95% yield). ¹H NMR (400 MHz, C₆D₆): δ 7.43-7.37 (m, 1H, ArH), 7.14-7.05 (m, 4H, ArH), 6.97-6.91 (m, 1H, ArH), 6.38 (ddd, *J*= 7.9, 5.2, 2.4 Hz, 4H, ArH), 6.34-6.29 (m, 4H, ArH), 3.46 (s, 6H, -OCH₃), 3.37 (s, 6H, -OCH₃), 3.21 (s, 6H, -OCH₃), 3.16 (s, 6H, -OCH₃), 2.15-2.05 (m, 2H, -PCH₂-), 2.00-1.89 (m, 2H, -PCH₂-), 1.81-1.70 (m, 1H, -PCH₂-), 1.67-1.57 (m, 1H, -PCH₂-), 1.41 (s, 9H, -OC(CH₃)₃), 1.35 (dt, *J*= 15.2, 7.6 Hz, 9 H, -PCH₂CH₃), 1.18-1.12 (Overlapping m+s (1.15), 11H, -C(CH₃)₃ + -NiCHRCH₂CH₃), 0.93-0.81 (Overlapping, 4H, -NiCHRCH₂CH₃). ¹³C{¹H} NMR (101 MHz, C₆D₆): δ 163.81 (d, *J*= 8.3 Hz, 4C, Aryl-C), 162.48 (s, 4C, Aryl-C), 162.15 (s, 2C, Aryl-C), 133.44 (d, *J*= 6.5 Hz, 1C, Aryl-C), 131.42 (s, 1C, Aryl-C), 130.10 (d, *J*_{CP}= 7.7 Hz, 2C, Aryl-C), 128.96 (s, 2C, Aryl-C), 128.58 (d, 2C, Aryl-C), 125.66 (broad s, 2C, Aryl-C), 121.96 (d, *J*_{CP}= 96.8 Hz, 1C, Aryl-C), 118.87 (d, *J*_{CP}= 35.3 Hz, 1C, Aryl-C), 118.52 (d, *J*_{CP}= 39.8 Hz, 1C, Aryl-C), 105.48 (s, 2C, Aryl-C), 105.29 (s, 2C, Aryl-C), 104.01 (s, 1C, -OC(CH₃)₃), 75.98 (s, 2C, Acyl-C), 55.91 (s, 2C, Aryl-C), 55.80 (s, 2C, Aryl-C), 55.60 (s, 2C, Aryl-C), 55.30 (s, 2C, Aryl-C), 34.02 (s, 1C, -C(CH₃)₃), 32.31 (s, 3C, -C(CH₃)₃), 28.81 (s, 3C, -OC(CH₃)₃), 25.32 (s, 1C, -PCH₂-), 19.92 (s, 1C, Ni-).

$\text{CHRCH}_2\text{CH}_3$), 16.24 (s, 1C Ni- $\text{CHRCH}_2\text{CH}_3$), 14.56 (s, 1C, - PCH_2-), 14.37 (s, 1C, - PCH_2-), 8.99 (broad s, 3C, - PCH_2CH_3), 5.93 (s, 1C, Ni- $\text{CHRCH}_2\text{CH}_3$). $^{31}\text{P}\{\text{H}\}$ NMR (162 MHz, C_6D_6 , 298 K): δ 11.65 (d, $J_{\text{PP}} = 291.3$ Hz, 1P), -12.01 (dd, $J_{\text{PP}} = 291.3$ Hz, 11.2, 1P), -51.76 (d, $J_{\text{PP}} = 11.2$ Hz, 1P). Anal. Calcd(%) for $\text{C}_{56}\text{H}_{77}\text{NiO}_{11}\text{P}_3$: C: 62.40, H: 7.20; found: C: 63.28, H: 6.78.

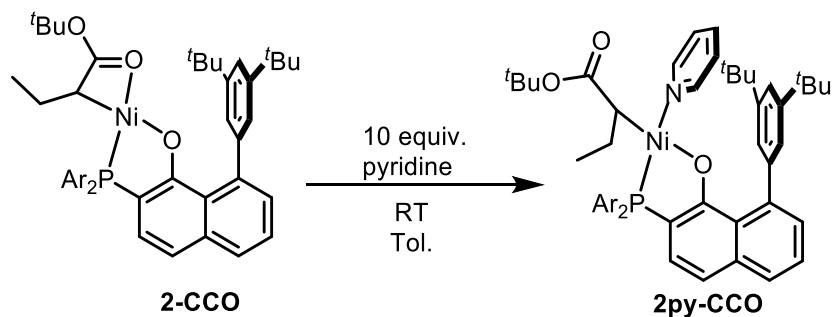


2et-CCO: A solution of complex **2-CCO** (5.6 mg, 0.0067 mmol) in C_7D_8 (0.6 mL) was prepared in the glovebox and transferred to a J-Young NMR tube. The J-Young NMR tube and a calibrated gas bulb (33.93 mL) were connected to a high-vacuum line. Dinitrogen in the J-Young tube was removed by three freeze-pump-thaw cycles of five minutes each. A separate vessel containing ethylene was connected to the high-vacuum line, cooled with liquid nitrogen, and placed under vacuum to remove residual dioxygen. The liquid nitrogen Dewar was then removed and ethylene was slowly transferred to the calibrated gas bulb. The calibrated gas bulb was sealed once the manometer read a pressure of 224 Torr. The ethylene in the calibrated gas bulb was then condensed in the J-Young NMR tube by cooling with liquid nitrogen over a period of 3 minutes. The J-Young NMR tube was then transferred to a dry-ice acetone bath and subsequently inserted to a pre-cooled NMR probe. Complex **2et-**

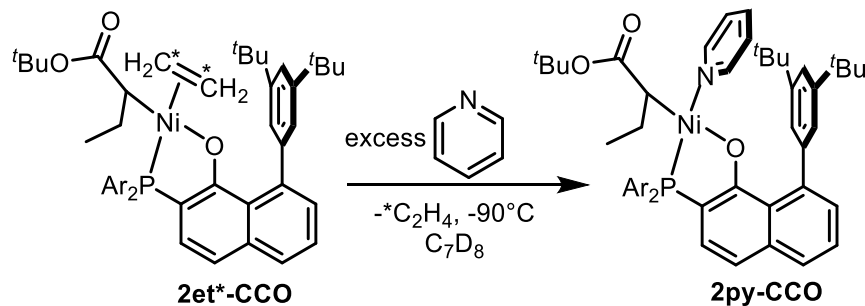
CCO was characterized by $^{31}\text{P}\{\text{H}\}$ NMR. $^{31}\text{P}\{\text{H}\}$ NMR (121 MHz, C_6D_6 , 183 K): δ -19.60 (broad s, 1P).



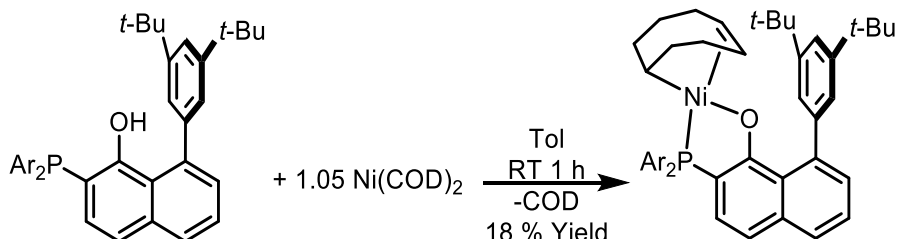
2et*-CCO: A similar protocol to generating **2et-CCO** was performed to characterize **2et*-CCO**, using $^{13}\text{C}_2\text{H}_4$ ethylene. Complex **2et*-CCO** was partially characterized by $^{13}\text{C}\{\text{H}\}$, and $^{31}\text{P}\{\text{H}\}$ NMR. $^{31}\text{P}\{\text{H}\}$ NMR (121 MHz, C_7D_8 , 183 K): δ -19.60 (broad s, 1P). $^{13}\text{C}\{\text{H}\}$ NMR (101 MHz, C_7D_8 , 183 K): δ 99.00 (broad d, 1C, $^1J_{\text{CC}} = 48.2$ Hz, $^{13}\text{C}_2\text{H}_4$) 95.46 (broad d, 1C, $^1J_{\text{CC}} = 48.2$ Hz, $^{13}\text{C}_2\text{H}_4$).



2py-CCO: To a solution of **2-CCO** (50 mg, 0.06 mmol) in 4 mL of diethyl ether in a 20 mL scintillation vial in the glovebox was added 10 equivalents of pyridine (80 mg, 0.06 mmol) in diethyl ether, affording quantitative generation of **2py-CCO**. ^1H NMR (400 MHz, C_6D_6 , 298 K) $^{31}\text{P}\{\text{H}\}$ NMR (121 MHz, C_6D_6 , 298 K): δ -19.60 (broad s, 1P)



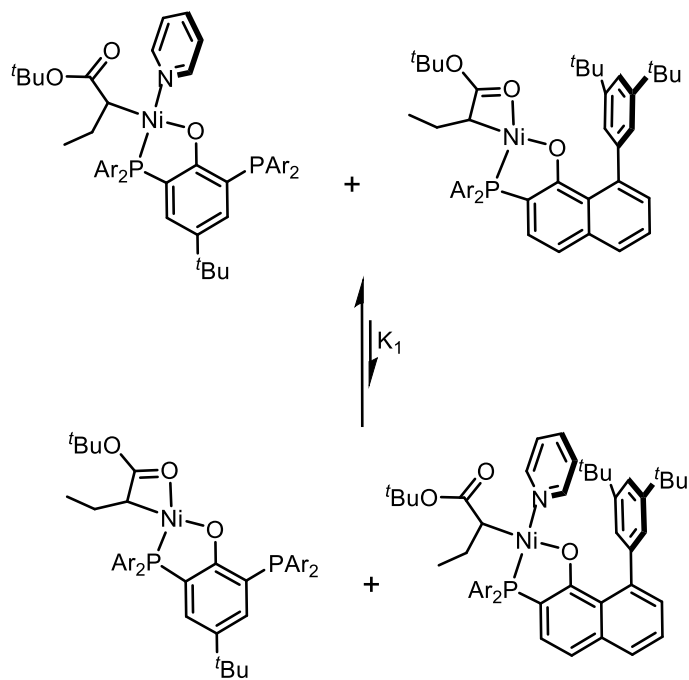
Conversion of Olefin Adduct **2et^{*}-CCO to **2py-CCO**:** The previously characterized sample of **2et^{*}-CCO** in a J-young tube was frozen in a liquid nitrogen Dewar and attached to the high vacuum line. A Schlenk tube of pyridine was also attached to the high vacuum line and an excess of pyridine was vacuum transferred to the sample of **2et^{*}-CCO** over a period of 10 minutes. The J-young tube was then sealed, thawed in a dry ice-acetone bath and transferred to the precooled NMR spectrometer probe. The NMR experiments showed the displacement of ethylene as indicated by the disappearance of ³¹P and ¹³C resonances corresponding to **2et^{*}-CCO** for both the bound phosphine ligand and the bound ethylene.



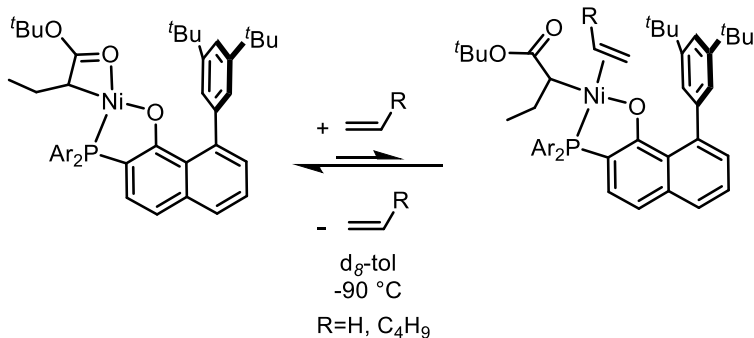
2-C₈H₁₃: In the glove box, to a solution of Ni(COD)₂ (35 mg, 0.125 mmol) in toluene (5 ml) in a vial was added a solution of **PONap-H** (80 mg, 0.125 mmol) in toluene (2 ml). The mixture was stirred for 2 h under room temperature, forming a dark yellow solution. Volatile materials were removed under vacuum and triturated with n-hexanes three times. The residue was washed with n-pentane and cold diethyl ether and subsequently was extracted with benzene and dried in vacuo to provide the complex **2-C₈H₁₃** (78 mg, 76%) as a yellowish

solid. ^1H NMR (400 MHz, C_6D_6): δ 7.82(dd, $^3J_{\text{HH}} = 8.4$ Hz, $^3J_{\text{HH}} = 9.2$ Hz, 1H, PhH), 7.66(dd, $^3J_{\text{HH}} = 7.9$ Hz, $^4J_{\text{HH}} = 1.8$ Hz, 1H, PhH), 7.57(t, $^4J_{\text{HH}} = 1.9$ Hz 1H, PhH), 7.30(apparent t, $^4J_{\text{HH}} = 1.6$ Hz, 1H, ArH), 7.21-7.28(overlapping multiplets, 2H, ArH), 6.26(dd, $^3J_{\text{HH}} = 8.2$ Hz, $^4J_{\text{HP}} = 3.3$ Hz, 2H, PhH), 6.22(dd, $^3J_{\text{HH}} = 8.2$ Hz, $^4J_{\text{HP}} = 3.3$ Hz, 2H, PhH), 5.47(multiplet, 1H, olefinic-CH), 5.19(multiplet, 1H, olefinic H) 3.42(s, 6H, OCH_3), 3.04(s, 6H, OCH_3), 2.21(multiplet, 4H, aliphatic-H), 1.93(multiplet, 2H, aliphatic-H), 1.47(s, 9H, $\text{O}'\text{Bu}$), 1.48(s, 9H, tBu), 1.42(s, 9H, tBu), 0.78-1.60(overlapping multiplets, 4H, aliphatic H), 0.22(doublet of multiplets, $^3J_{\text{HP}} = 14.2$ Hz, 1H, Ni-CH). $^{13}\text{C}\{\text{H}\}$ NMR (101 MHz, C_6D_6): δ 172.61(d, $J_{\text{CP}} = 27.5$ Hz, 1C, Aryl-C), 161.97(d, $J_{\text{CP}} = 2.0$ Hz, 1C, Aryl-C), 161.86(d, $J_{\text{CP}} = 2.0$ Hz, 1C, Aryl-C), 147.93(s, 1C, Aryl-C), 147.72(s, 1C, Aryl-C), 147.31(s, 1C, Aryl-C), 143.05(d, $J_{\text{CP}} = 2.8$ Hz, 1C, Aryl-C), 138.45(d, $J_{\text{CP}} = 2.8$ Hz, 1C, Aryl-C), 129.88(d, $J_{\text{CP}} = 11.5$ Hz, 1C, Aryl-C), 129.51(d, $J_{\text{CP}} = 2.5$ Hz, 1C, Aryl-C), 128.22(s, 1C, Aryl-C), 126.97(s, 1C, Aryl-C), 127.09(s, 2C, Aryl-C), 126.63(s, 1C, Aryl-C), 125.13(s, 2C, Aryl-C), 122.75(s, 1C, Aryl-C), 122.57(s, 1C, Aryl-C), 118.92(s, 1C, Aryl-C), 114.33(d, $J_{\text{CP}} = 60.1$ Hz, 1C, Aryl-C), 113.53(d, $J_{\text{CP}} = 42.4$ Hz, 1C, Aryl-C), 111.76(d, $J_{\text{CP}} = 7.2$ Hz, 1C, Aryl-C), 109.30(d, $J_{\text{CP}} = 42.4$ Hz, 1C, Aryl-C), 104.91 (d, $J_{\text{CP}} = 3.6$ Hz, 1C, Aryl-C), 104.64(d, $J_{\text{CP}} = 2.7$ Hz, 1C, olefinic-C), 104.91(d, $J_{\text{CP}} = 3.6$ Hz, 1C, Aryl-C), 104.20(d, $J_{\text{CP}} = 4.0$ Hz, 1C, Aryl-C), 101.74(d, $J_{\text{CP}} = 12.8$ Hz, 1C, olefinic-C), 56.75(s, 2C, $\text{OC}(\text{CH}_3)_3$), 55.14(s, 2C, OCH_3), 39.91(d, 1C, $^2J_{\text{CP}} = 5.2$ Hz, aliphatic-C), 35.45 (s, 1C, aliphatic-C), 34.96(d, $^2J_{\text{CP}} = 12.0$ Hz, 1C, Ni-CH), 32.16(s, 3C, $\text{CH}(\text{CH}_3)_3$), 32.00(s, 3C, $\text{CH}(\text{CH}_3)_3$), 31.74(s, 3C, $\text{CH}(\text{CH}_3)_3$), 30.29(s, 1C, aliphatic-C), 27.86(s, 1C, aliphatic-C), 20.06(d, $^3J_{\text{CP}} = 3.3$ Hz, 1C, Ni- CHCH_2), 25.99(multiplet, 1C, aliphatic C), 22.96(s, 1C, aliphatic C), 22.79(s, 1C, aliphatic C); $^{31}\text{P}\{\text{H}\}$ NMR (121 MHz,

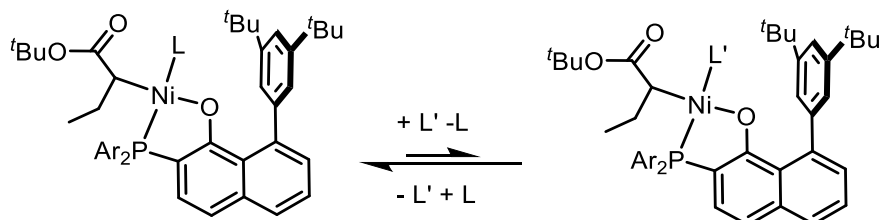
C_6D_6 , 298 K): δ -19.61(s, 1P, Ni-PONap). Anal. Calcd(%) for $\text{C}_{48}\text{H}_{57}\text{NiO}_5\text{P}$: C: 71.74, H: 7.15; found: C: 72.03, H: 7.33.



Pyridine Exchange Between **1L-CCO and **2L-CCO**:** A solution of **2-CCO** (8.4 mg, 0.01 mmol) in d6-benzene was transferred to a 20 mL scintillation vial in the glovebox with one equivalent of **1py-CCO** (10.4 mg, 0.01 mmol). The mixture was fully dissolved and transferred to a NMR tube after 0.5 hours. The four species, **1-CCO**, **1py-CCO**, **2-CCO**, and **2py-CCO** were identified by $^{31}\text{P}\{\text{H}\}$ NMR. The solution was monitored by NMR until relative intensities of the four species were unchanged, indicating equilibrium has been reached. Relative intensities of the four species were modelled indicating a K value of 8.0×10^{-2} and ΔG of 1.5 kcal/mol.

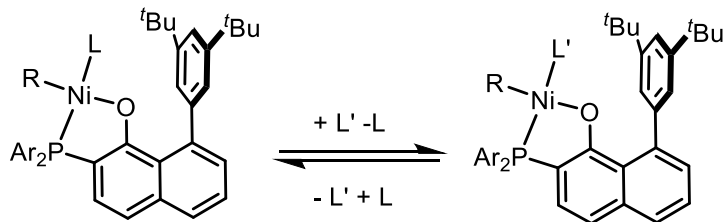


Quantitative determination of ring opening thermodynamics of 2-CCO by olefins: In the glovebox, to a solution of 2-CCO (6.3 mg, 0.0075 mmol) and internal standard hexamethyldisiloxane (6.8 mg, 0.0419 mmol) in d8-toluene (637 mg) was added an excess of olefin (ethylene or 1-hexene) at -78°C . The solution was transferred to a precooled NMR probe and NMR spectra were recorded. The probe was then warmed to -10°C to allow the mixture to reach a thermodynamic equilibrium while hindering migratory insertion from proceeding. The mixture was recooled to -90°C and NMR spectra were recollected. This process was repeated until the relative intensities of the starting material and the olefin coordination compounds were unchanged. The relative intensities by $^{31}\text{P}\{\text{H}\}$ NMR spectra were used to calculate the K values of 3.0×10^{-1} and 5.5×10^{-3} and the ΔG of 0.4 kcal/mol and 1.9 kcal/mol for ethylene and 1-hexene, respectively.



Thermodynamics of ligand exchange with pyridines and olefins at 183 K: A similar procedure to the above quantitative determination of thermodynamic binding constants was adapted to determine the relative thermodynamic binding constant between lutidine and ethylene. In order to determine the K value between pyridine and ethylene coordinated adduct

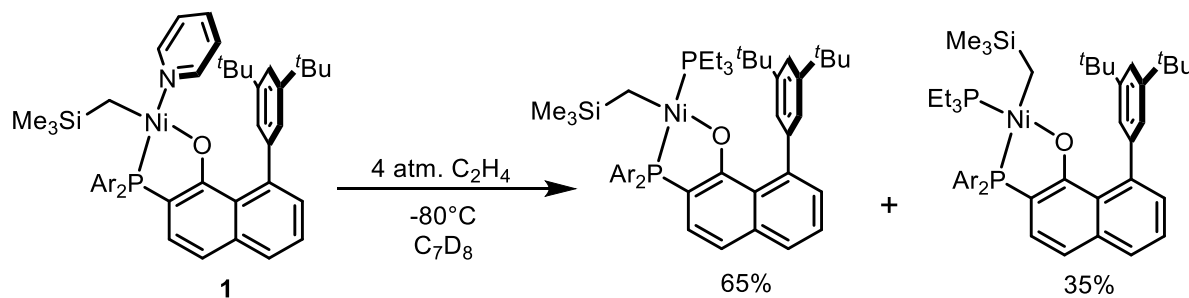
to be 1.1×10^{-4} and a ΔG value of 1.4 kcal/mol, the K value for **2lut-CCO** and **2py-CCO** was determined by mixing **2-CCO** (5.1 mg, 0.0061 mmol), lutidine (72 mg, 0.67 mmol) and pyridine (7.5 mg, 0.0948 mmol). The mixture was cooled to 183 K and the relative intensities observed in the $^{31}\text{P}\{^1\text{H}\}$ NMR spectrum was used to determine the K value of 4.8×10^{-3} and a ΔG value of 1.9 kcal/mol. These combined results allow the quantitative determination of the K value between pyridine and ethylene coordinated adducts of 1.1×10^{-4} and a ΔG value of 3.3 kcal/mol.



Quantitative determination of thermodynamics of ligand exchange for non-olefin donors: In the glovebox, to a solution of 2L-R (0.0122 mmol) and internal standard of hexamethyldisiloxane in C₆D₆ (406 mg) was added a known amount of a secondary ligand. The mixture was fully dissolved and transferred to an NMR tube. $^{31}\text{P}\{^1\text{H}\}$ and ^1H NMR spectra were collected in 20-minute intervals until the spectra were unchanged. The relative ratios were determined in one of two methods depending on the rate of exchange relative to the NMR timescale.

Method A. The rate of exchange is slow relative to the NMR timescale which lead to two separate species observed. The relative intensities of the two species are determined either by integration of Ni-CHR resonance in the ^1H NMR spectra or through the $^{31}\text{P}\{^1\text{H}\}$ NMR resonances.

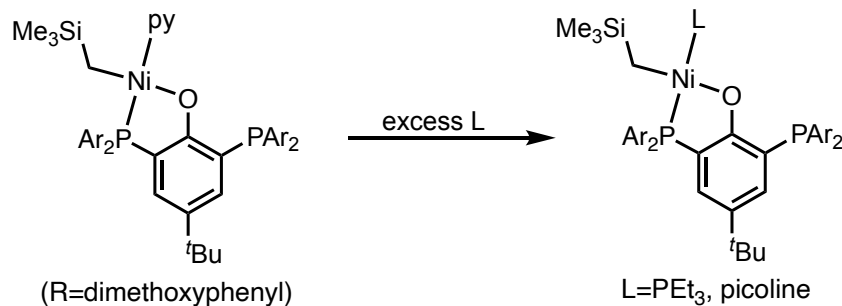
Method B. The rate of exchange is fast relative to the NMR timescale which precludes the observation of two sets of resonances for the mixture of species. The relative intensities of the two species are determined by comparing the resonances of the purified species and analyzing the separation of the methoxy resonance either of the ligand with different mixtures of both ligands.



2P: In the glovebox, to a stirring solution of 2 (7.2 mg, 0.0085 mmol) in toluene (2 mL) was added 40 equivalents of PEt₃ (40 mg, 0.034 mmol). The solution was stirred for 0.5 h and all volatiles were removed in vacuo. The resultant solid was triturated with hexanes (3 x 3 mL) and extracted with 5 mL of toluene, filtered through a plug of celite and concentrated, affording quantitative formation of 2P. Both ³¹P{¹H} and ¹H NMR suggest an approximate 2:1 mixture of the trans and cis isomer.

Trans isomer ¹H NMR (400 MHz, C₆D₆): δ 6.90-7.82 (overlapping multiplets with cis isomer, aromatic-H), 6.33 (dd, ³J_{HH} = 8.2 Hz, ⁴J_{HP} = 3.2 Hz, 4H, PhH), 3.31 (s, 12H, OCH₃), 1.38 (s, 18H, O'Bu), 1.20 (multiplet, 6H, Ni-CH₂-CH₃), 0.99 (dt, ³J_{HH} = 7.3 Hz, ³J_{HP} = 14.2 Hz, 9H, Ni-CH₂-CH₃), 0.11 (s, 9H, SiMe₃), -0.80 (apparent t (dd), ²J_{HP} = 12.7 Hz, 2H, Ni-CH₂); ³¹P{¹H} NMR (121 MHz, C₆D₆, 298 K): δ 12.09(d, ²J_{PP} = 325.2 Hz, 1P), -13.84(d, ²J_{PP} = 325.2 Hz, 1P);

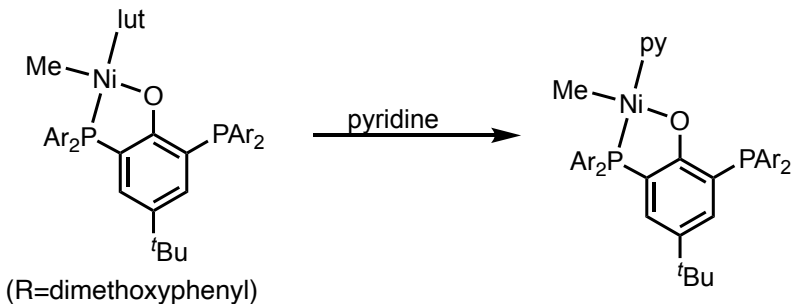
Cis Isomer: ^1H NMR (400 MHz, C_6D_6): δ 6.90-7.82 (overlapping multiplets with cis isomer, aromatic-H), 6.23 (dd, $^3J_{\text{HH}} = 8.2$ Hz, $^4J_{\text{HP}} = 3.2$ Hz, 4H, PhH), 3.18 (s, 12H, OCH_3), 1.60 (s, 18H, $\text{O}'\text{Bu}$), 1.43 (overlapping multiplet, 6H, Ni- $\text{CH}_2\text{-CH}_3$), 0.80 (dt, $^3J_{\text{HH}} = 7.5$ Hz, $^3J_{\text{HP}} = 14.6$ Hz, 9H, Ni- $\text{CH}_2\text{-CH}_3$), 0.22 (s, 9H, SiMe_3), -0.02 (broad multiplet, $W_{1/2} = 18$ Hz, 2H, Ni- CH_2); $^{31}\text{P}\{\text{H}\}$ NMR (121 MHz, C_6D_6 , 298 K): δ 18.06 (d, $^2J_{\text{PP}} = 19.6$ Hz, 1P), -8.91 (d, $^2J_{\text{PP}} = 19.6$ Hz, 1P);



1P: In the glove box, to a solution of **1** (29.6 mg, 0.03 mmol) in toluene (1.5 mL) was added 1 equiv. of PEt_3 (3.5 mg, 0.03 mmol). The mixture was stirred for 10 min under room temperature, forming a red solution. After removal of volatiles, additional 1 equiv. of PEt_3 (3.5 mg, 0.03 mmol) and toluene (1.5 mL) was added to the residue. After stirring for 10 min, the volatiles were removed once again and the residue was triturated with pentane three times, forming the desired product as a red-orange solid (28.8 mg, 94%). ^1H NMR (400 MHz, C_6D_6) of the major isomer: δ 7.45 (dd, $^3J_{\text{HP}} = 10.4$ Hz, $^4J_{\text{HH}} = 2.4$ Hz, 1H, PhH), 7.31 (broad s, 1H, PhH), 7.08–7.02 (m, 4H, PhH), 6.37 (dd, $^3J_{\text{HH}} = 8.0$ Hz, $^4J_{\text{HH}} = 2.4$ Hz, 4H, PhH), 6.27 (dd, $^3J_{\text{HH}} = 8.0$ Hz, $^4J_{\text{HH}} = 3.2$ Hz, 4H, PhH), 3.31 (s, 12H, OCH_3), 3.20 (s, 12H, OCH_3), 1.22-1.14 (m, 6H, $\text{P}(\text{CH}_2\text{CH}_3)_3$), 1.13 (s, 9H, $\text{C}(\text{CH}_3)_3$), 1.09-1.06 (t, $^3J_{\text{HH}} = 7.2$ Hz, 9H, $\text{P}(\text{CH}_2\text{CH}_3)_3$), 0.15 (s, 9H, $\text{Si}(\text{CH}_3)_3$), -0.88–-0.94 (dd, $^3J_{\text{HP}} = 11.7$ Hz, $^3J_{\text{HP}} = 11.5$ Hz 2H, Ni- CH_2Si); $^{13}\text{C}\{\text{H}\}$ NMR (101 MHz, C_7D_8) of the major isomer: 164.31 (s, 2C, Ar-C), 164.19 (s, 2C, Ar-C),

162.31 (m, 2C, Ar-C), 133.44 (m, 1C, Ar-C), 131.60 (broad s, 1C, Ar-C), 130.37 (s, 4C, Ar-C), 126.49 (s, 2C, Ar-C), 105.82 (s, 8C, Ar-C), 104.51 (s, 4C, Ar-C), 104.47 (s, 4C, Ar-C), 56.18 (s, 4C, OCH₃), 55.62 (s, 4C, OCH₃), 34.44 (s, 1C, C(CH₃)₃), 32.71 (s, 3C, C(CH₃)₃), 14.64 (m, C, P(CH₂CH₃)₃), 9.04 (m, C, P(CH₂CH₃)₃), 4.24 (s, 3C, SiMe₃), -26.37 (m, 1C, NiCH₂Si); ³¹P{¹H} NMR (121 MHz, C₆D₆) of the major isomer: δ 12.19 (d, ²J_{PP} = 197 Hz, 1P), -12.74 (d, ²J_{PP} = 197 Hz, ⁴J_{PP} = 7.1 Hz, 1P), -51.61 (d, ⁴J_{PP} = 7.1 Hz, 1P); ³¹P{¹H} NMR (121 MHz, C₆D₆) of the minor isomer: δ 21.02 (d, ²J_{PP} = 12.3 Hz, 1P), -3.35 (d, ²J_{PP} = 12.3 Hz, ⁴J_{PP} = 8.5 Hz, 1P), -50.37 (d, ⁴J_{PP} = 8.5 Hz, 1P). Anal. Calcd(%) for C₅₂H₇₃NiO₉P₃Si: C: 61.12, H: 7.20; found: C: 63.35, H: 6.76.

1pico: In the glove box, to a solution of **1** (19.6 mg, 0.02 mmol) in toluene (2 mL) was added 25 equiv. of 2-picoline (46.5 mg, 0.5 mmol). After stirred for 15 min, all volatiles were removed under vacuum. Twice more, 25 equiv. of 2-picoline was added to the residue with 2 mL toluene and volatiles were removed after stirring for 15 min, affording quantitative formation of **1pico** (19.5 mg, >95% yield). ¹H NMR (400 MHz, C₆D₆): δ 8.97 (d, ³J_{HH} = 5.6 Hz, 1H, PicoH), 7.46–7.39 (m, 1H, PhH), 7.31 (broad s, 1H, PhH), 7.08–7.05 (m, 4H, PhH), 6.96–6.93 (m, 1H, PhH), 6.77 (t, ³J_{HH} = 7.3 Hz, 1H, PicoH), 6.53 (d, ³J_{HH} = 7.3 Hz, 1H, PicoH), 6.42 (t, ³J_{HH} = 6.5 Hz, 1H, PicoH), 6.32 (d, ³J_{HH} = 8.4 Hz, 4H, PhH), 6.30 (d, ³J_{HH} = 8.4 Hz, 4H, PhH), 3.60 (s, 3H, pico-CH₃), 3.45–3.15 (m, 24H, OCH₃), 1.12 (s, 9H, C(CH₃)₃), -0.29 (s, 9H, Si(CH₃)₃), -1.39 (broad, 2H, NiCH₂Si); ³¹P{¹H} NMR (121 MHz, C₆D₆): δ -8.06 (d, ²J_{PP} = 10.5 Hz, 1P), -54.75 (d, ²J_{PP} = 10.5 Hz, 1P).



1py-Me: In the glove box, to a solution of **1lut-Me** (18.7 mg, 0.02 mmol) in toluene (2 mL) was added 15 equiv. of 2-picoline (23.7 mg, 0.3 mmol). After stirred for 15 min, all volatiles were removed under vacuum, affording quantitative formation of **1py-Me** (18.0 mg, >95% yield). ^1H NMR (400 MHz, C_6D_6): δ 8.59 (d, $^3\text{J}_{\text{HH}} = 5.4\text{Hz}$, 2H, PyH), 7.51 (dt, , $^3\text{J}_{\text{HP}} = 10.4\text{ Hz}$, $^4\text{J}_{\text{HH}} = 2.4\text{ Hz}$, 1H, PhH), 7.10–7.00 (m, 4H, PhH), 6.97 (m, 1H, PhH), 6.78 (t, $^3\text{J}_{\text{HH}} = 5.4\text{Hz}$, 1H), 6.41 (dd, $^3\text{J}_{\text{HH}} = 8.2\text{ Hz}$, $^4\text{J}_{\text{HH}} = 2.3\text{ Hz}$, 4H, PhH), 6.26 (dd, $^3\text{J}_{\text{HH}} = 8.3\text{ Hz}$, $^4\text{J}_{\text{HH}} = 3.4\text{ Hz}$, 4H, PhH), 3.34 (s, 6H, OCH_3), 3.25 (s, 12H, OCH_3), 1.15 (s, 9H, $\text{C}(\text{CH}_3)_3$), -0.49 (d, $^3\text{J}_{\text{HP}} = 5.8\text{ Hz}$, 3H, NiCH_3); $^{31}\text{P}\{\text{H}\}$ NMR (121 MHz, C_6D_6): δ -0.61 (d, $^2\text{J}_{\text{PP}} = 11.2\text{ Hz}$, 1P), -50.01 (d, $^2\text{J}_{\text{PP}} = 11.2\text{ Hz}$, 1P).

3. NMR Characterization

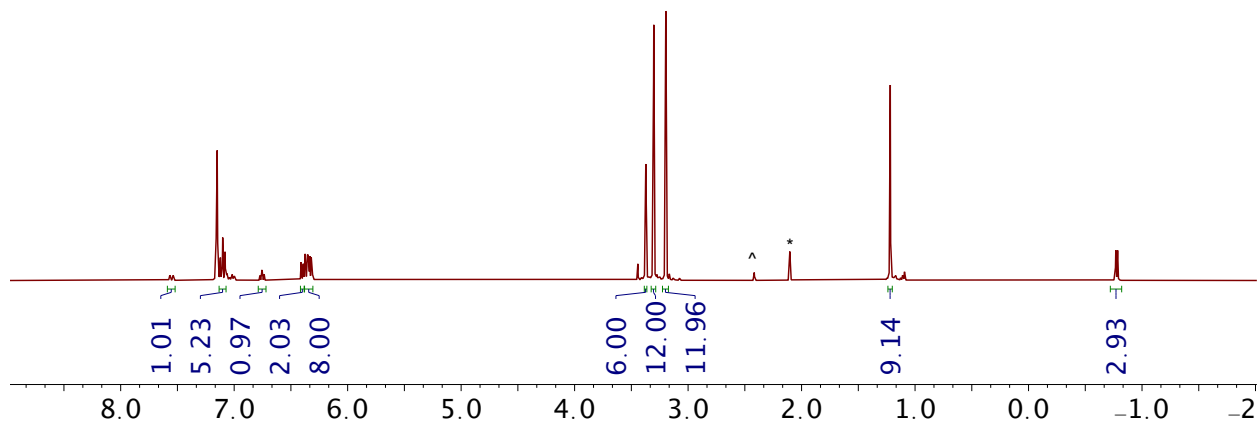


Figure S3.1. ^1H NMR of **1lut-Me** in C_6D_6 (*: residue toluene, ^: residue free lutidine)

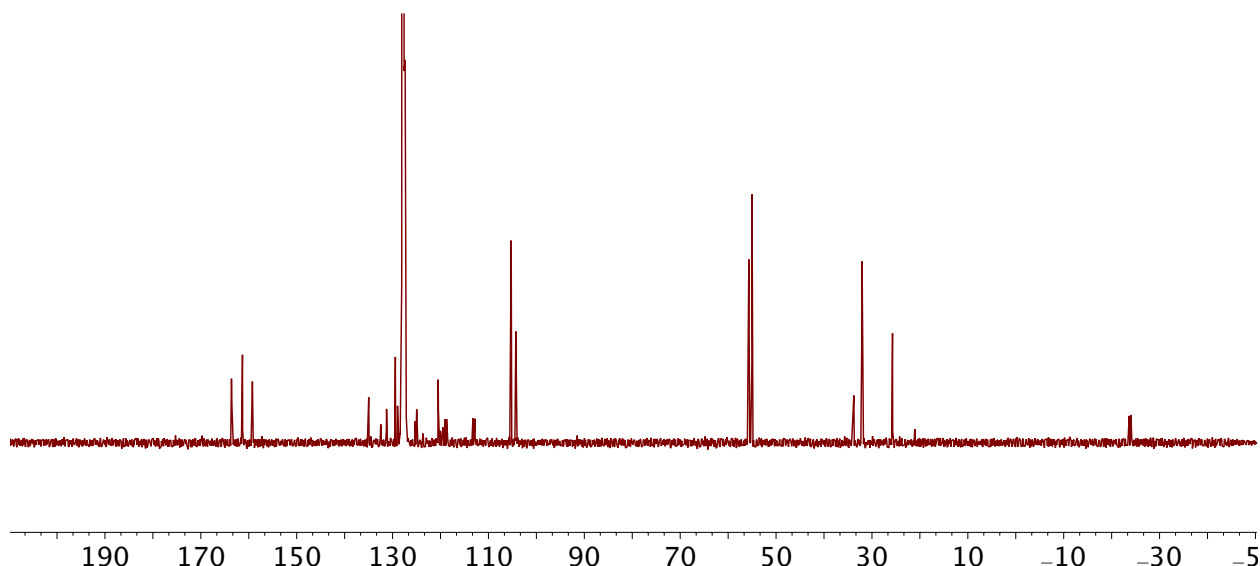


Figure S3.2. $^{13}\text{C}\{\text{H}\}$ NMR of **1lut-Me** in C_6D_6 .

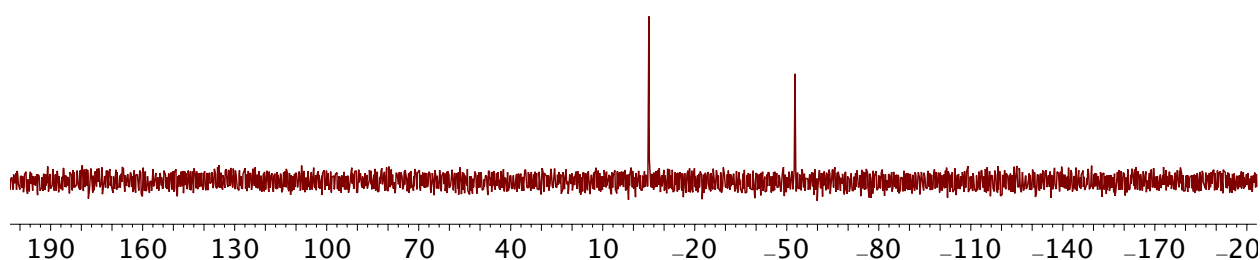


Figure S3.3. $^{31}\text{P}\{\text{H}\}$ NMR of **1lut-Me** in C_6D_6 .

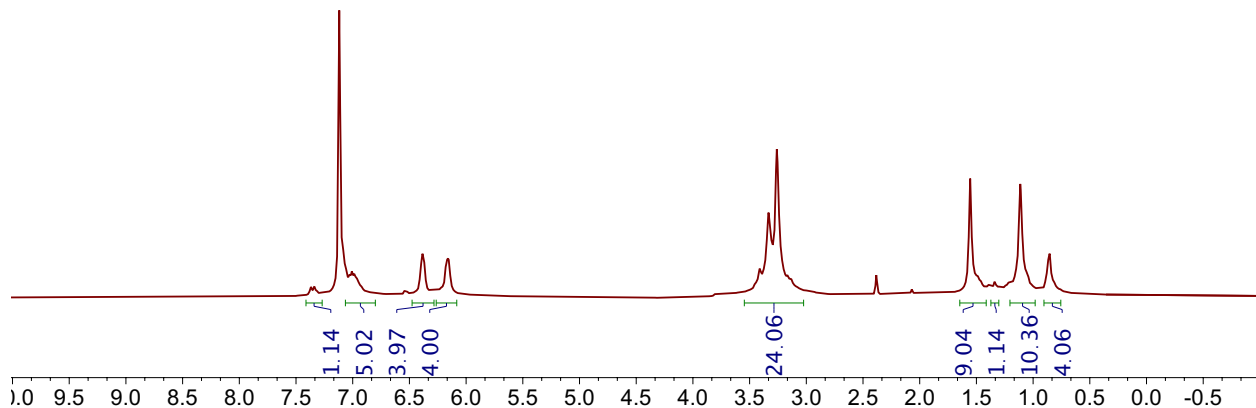


Figure S3.4. ^1H NMR of **2-CCO** in C_6D_6 .

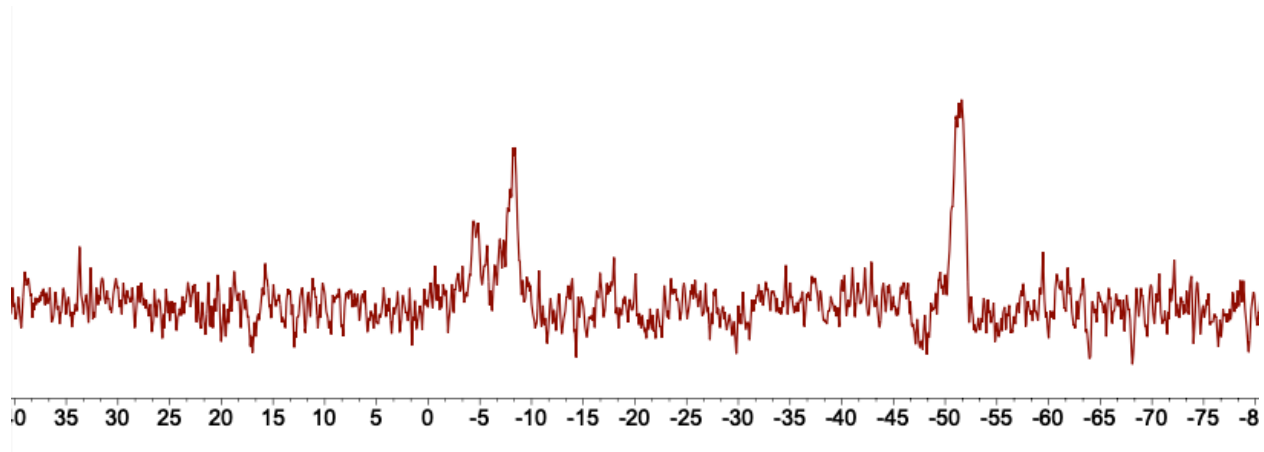


Figure S3.5. $^{31}\text{P}\{\text{H}\}$ NMR NMR of **2-CCO** in C_6D_6 .

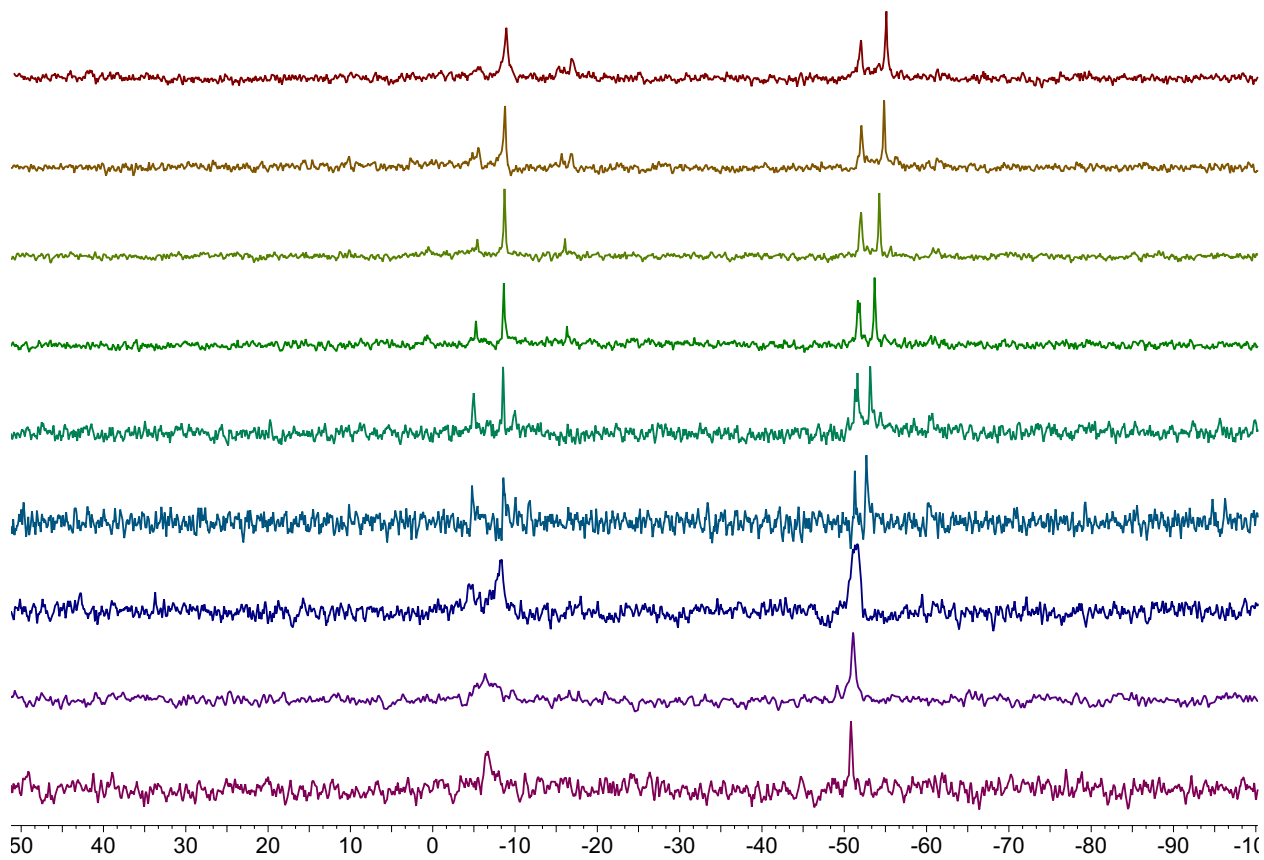


Figure S3.6. $^{31}\text{P}\{\text{H}\}$ NMR of **1-CCO** in Tol-d_8 at different temperatures (top to bottom: -90 °C, -60 °C, -40 °C, -20 °C, -0 °C, 25 °C, 40 °C, 60 °C).

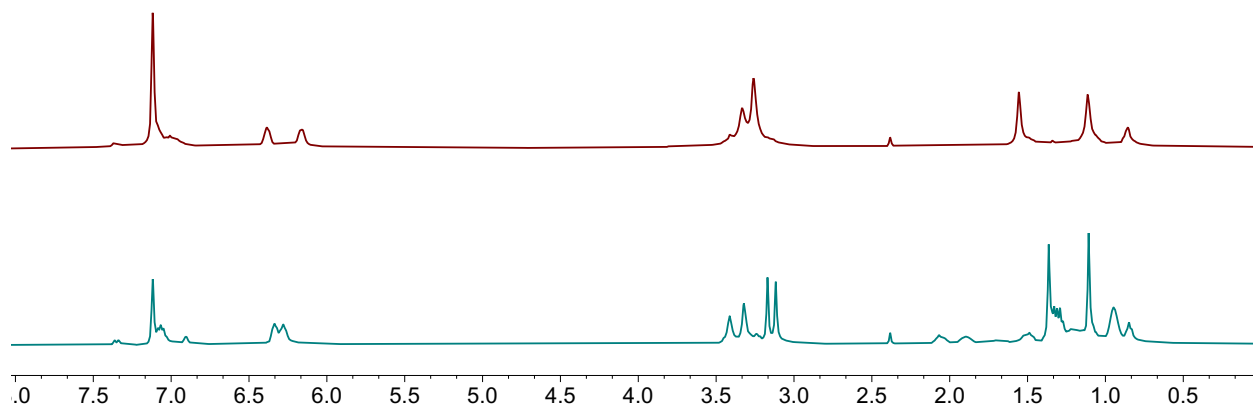


Figure S3.7. ^1H NMR Spectra of conversion of **1-CCO** (top) to **1P-CCO** (bottom) upon addition of PEt_3 .

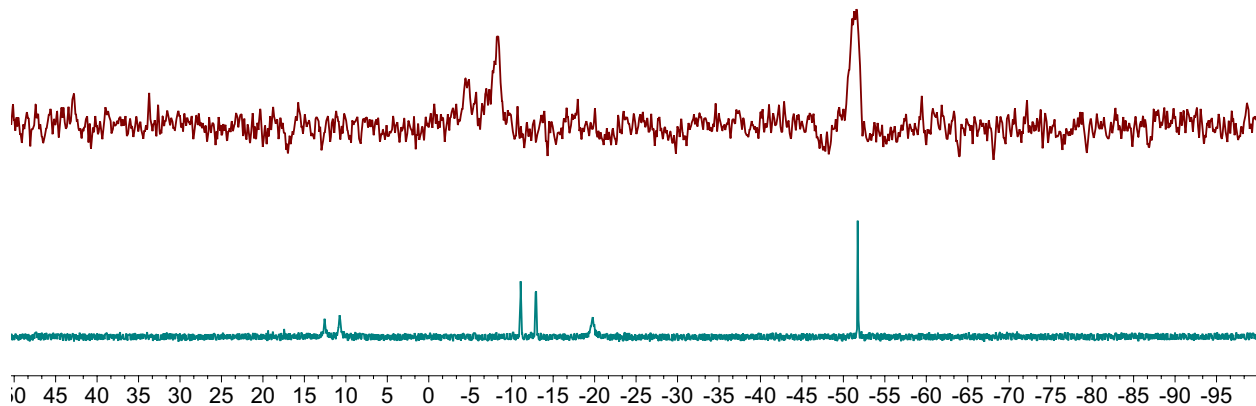


Figure S3.8. $^{31}\text{P}\{\text{H}\}$ NMR Spectra of conversion of **1-CCO** (top) to **1P-CCO** (bottom) upon addition of PEt_3 .

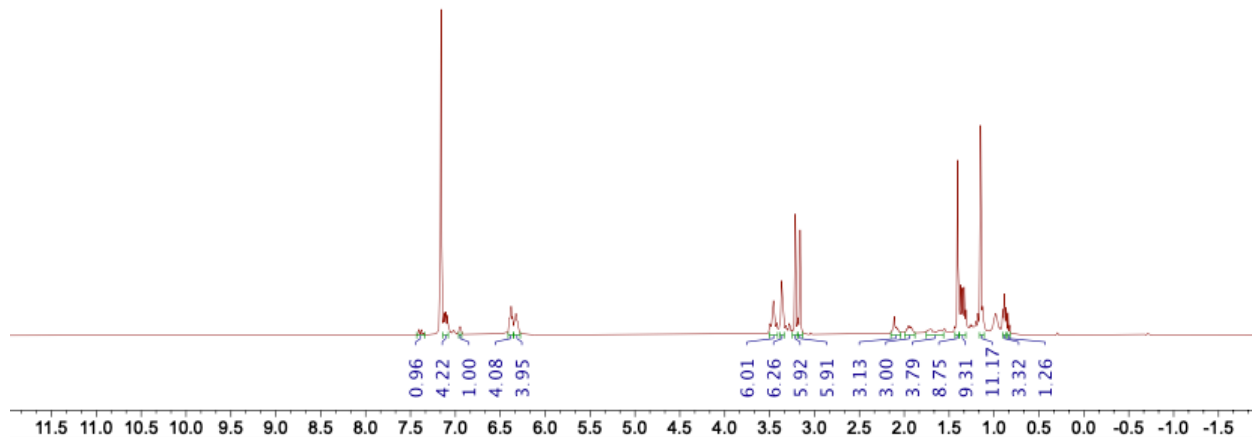


Figure S3.9. ^1H NMR of **1P-CCO** in C_6D_6 .

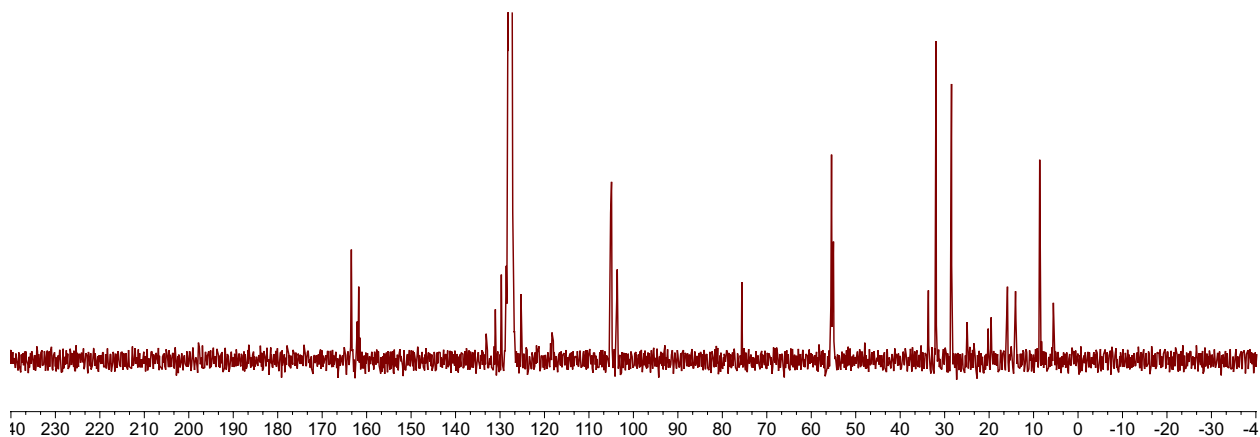


Figure S3.10. $^{13}\text{C}\{\text{H}\}$ NMR of **1P-CCO** in C_6D_6 .

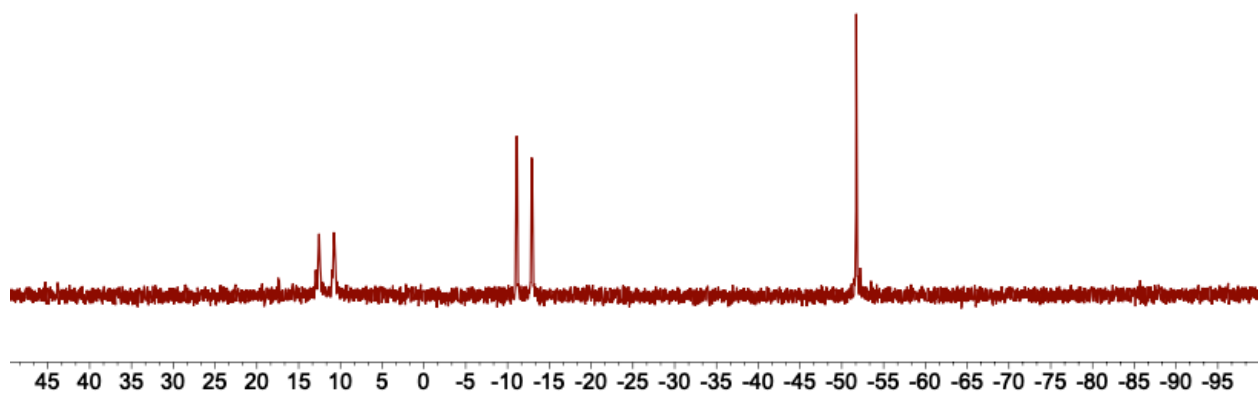


Figure S3.11. $^{31}\text{P}\{\text{H}\}$ NMR of **1P-CCO** in C_6D_6 .

Formation of **2et-CCO** from the addition of 4 atm. of ethylene to a solution of **2-CCO**

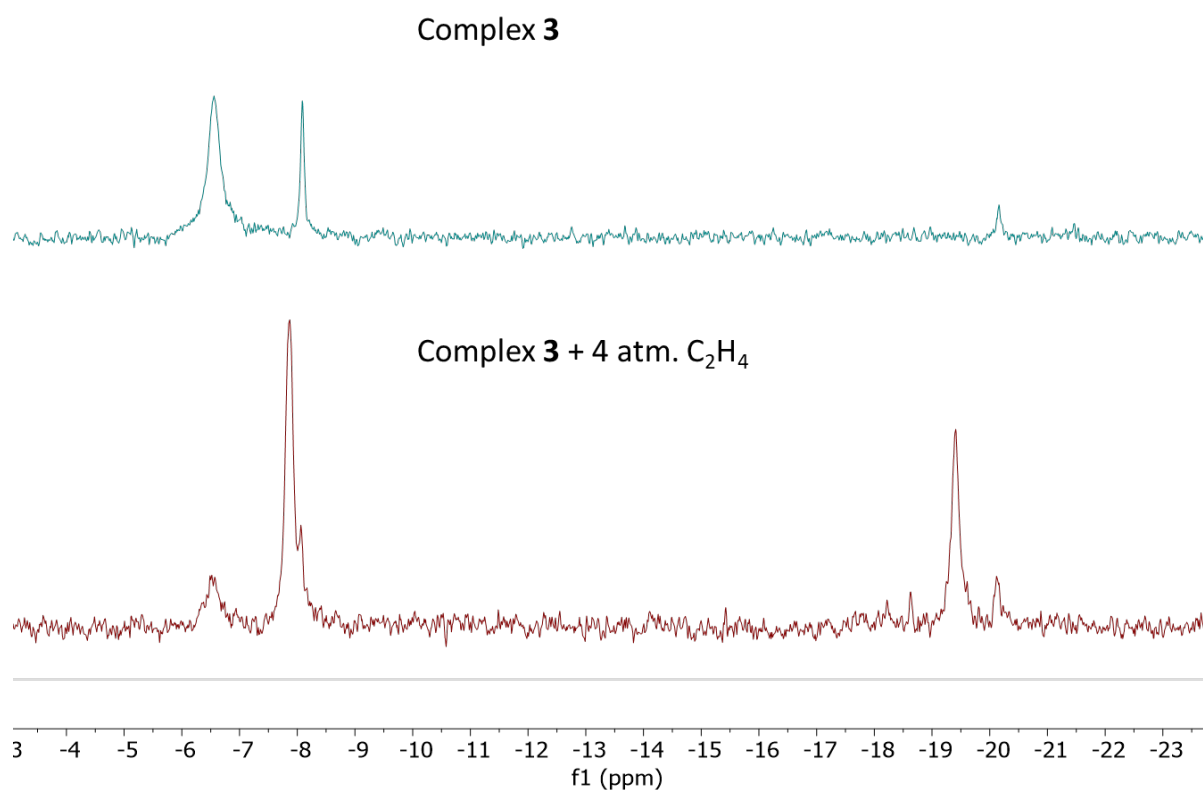


Figure S3.12 $^{31}\text{P}\{\text{H}\}$ NMR spectra of **2-CCO** (top) and **2-CCO** + 4 atm. ethylene (bottom)

(temperature: -80 °C, solvent: C₇D₈)

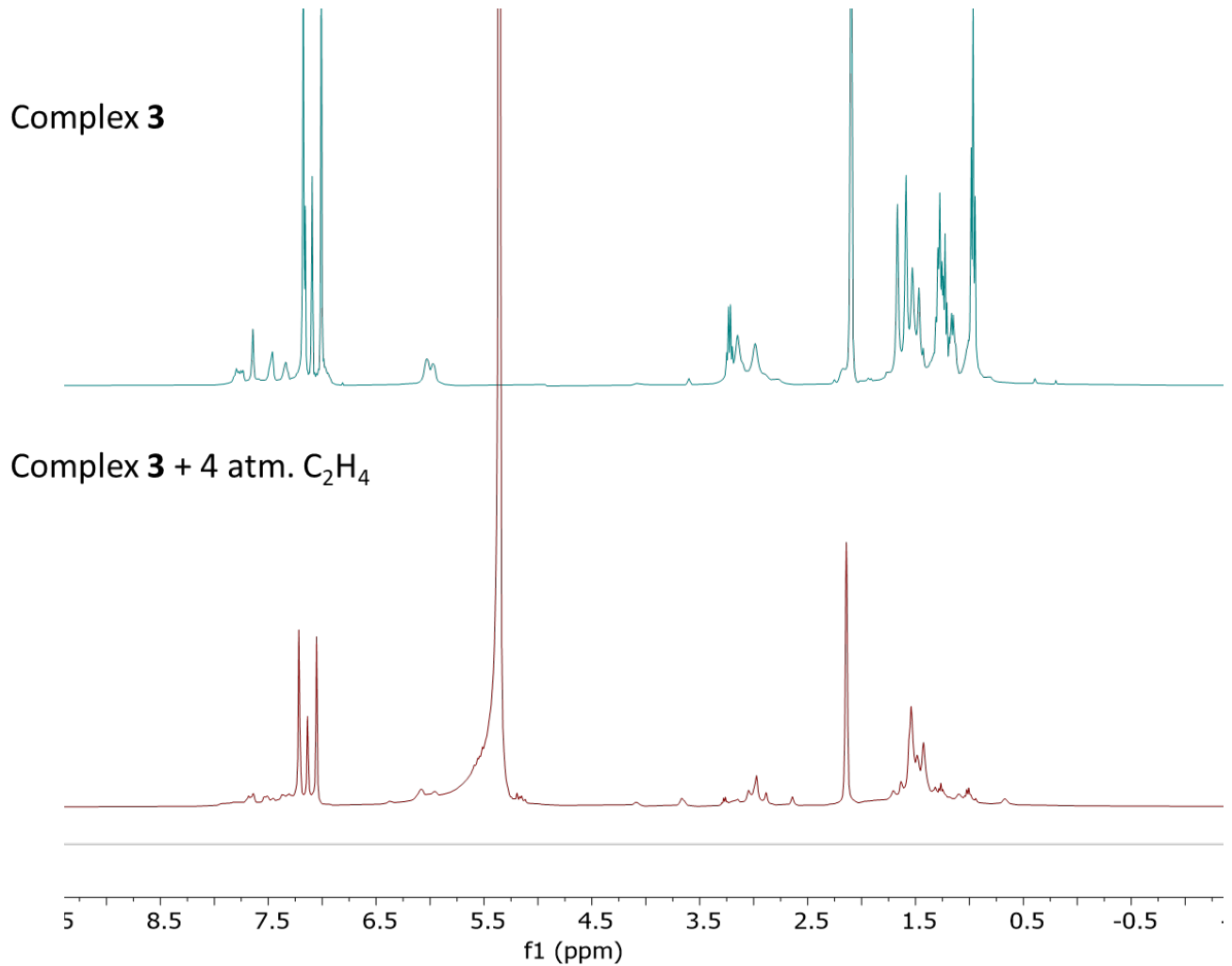


Figure S3.13 ¹H NMR spectra of **2-CCO** (top) and **2-CCO** + 4 atm. ethylene (bottom)

(temperature: -80 °C, solvent: C₇D₈)

$^{31}\text{P}\{\text{H}\}$ NMR showing formation of **2hex-CCO** from **2-CCO** and 1-hexene

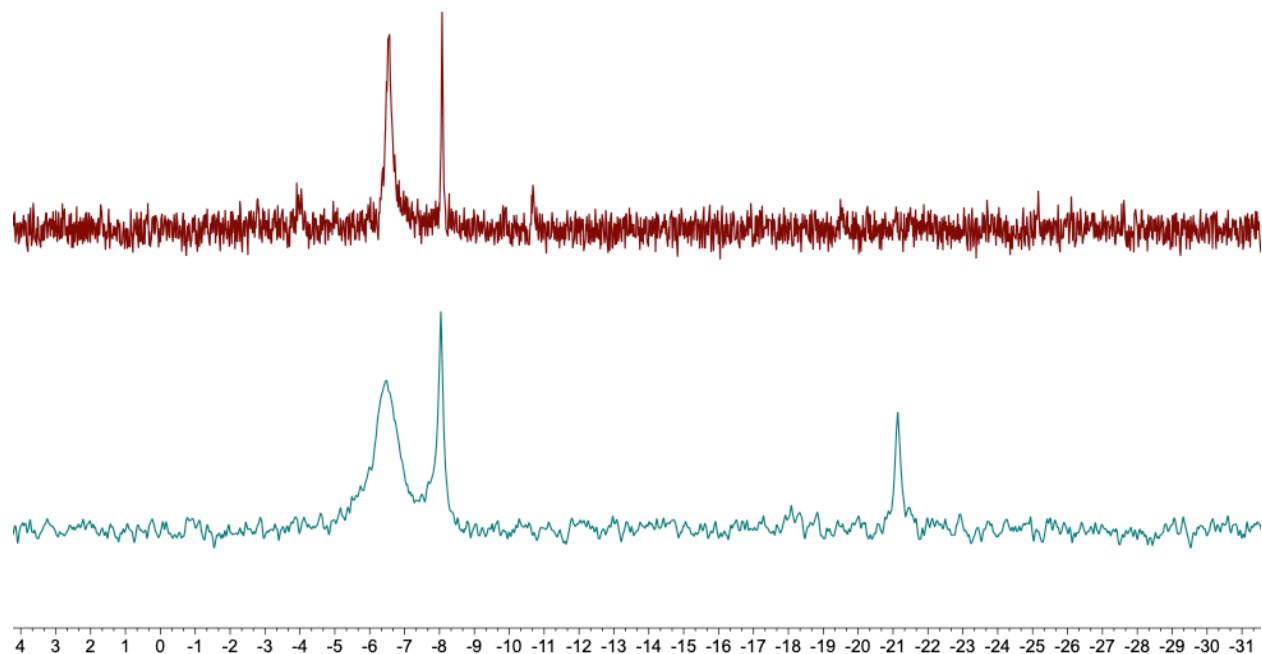


Figure S3.14 $^{31}\text{P}\{\text{H}\}$ NMR spectra of **2-CCO** (top) and **2-CCO + 200 equiv. of 1-hexene** (bottom) (temperature: $-80\text{ }^{\circ}\text{C}$, solvent: C_7D_8)

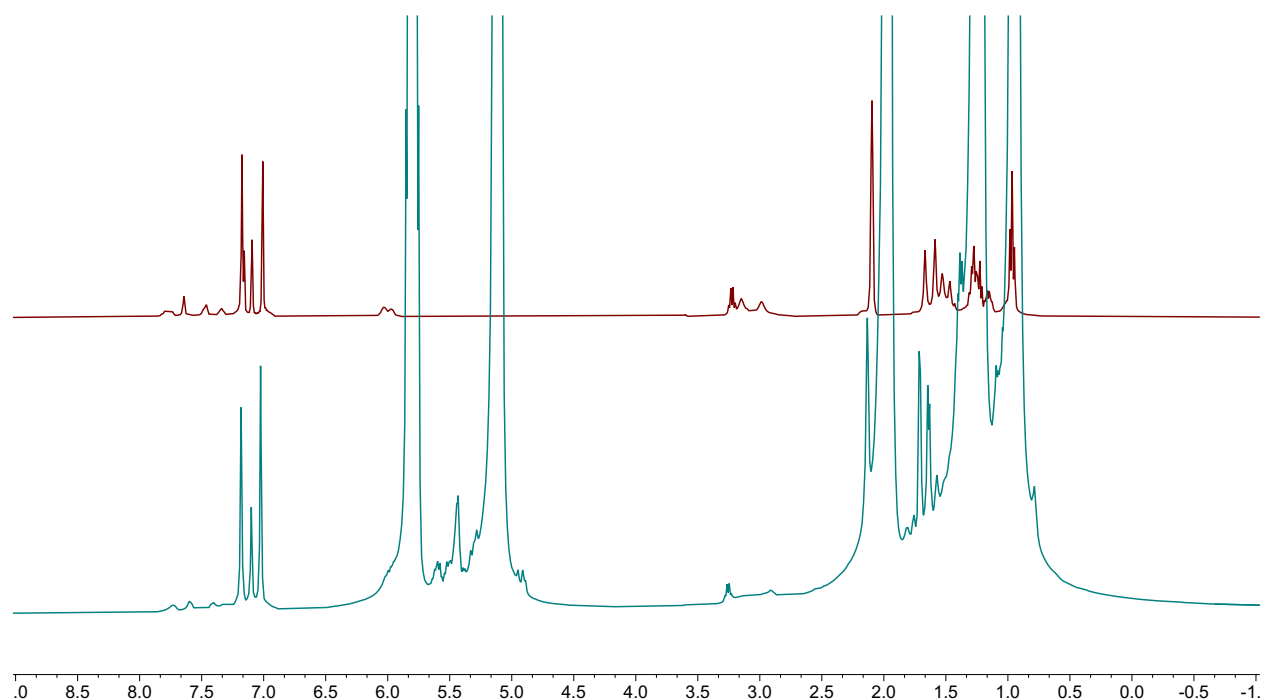


Figure S3.15 ^1H NMR spectra of **2-CCO** (top) and **2-CCO + 200 equiv. of 1-hexene** (bottom) (temperature: $-80\text{ }^{\circ}\text{C}$, solvent: C_7D_8)

Formation of **2et*-CCO** from the addition of 4 atm. of ^{13}C labelled ethylene to a solution of **2-CCO**

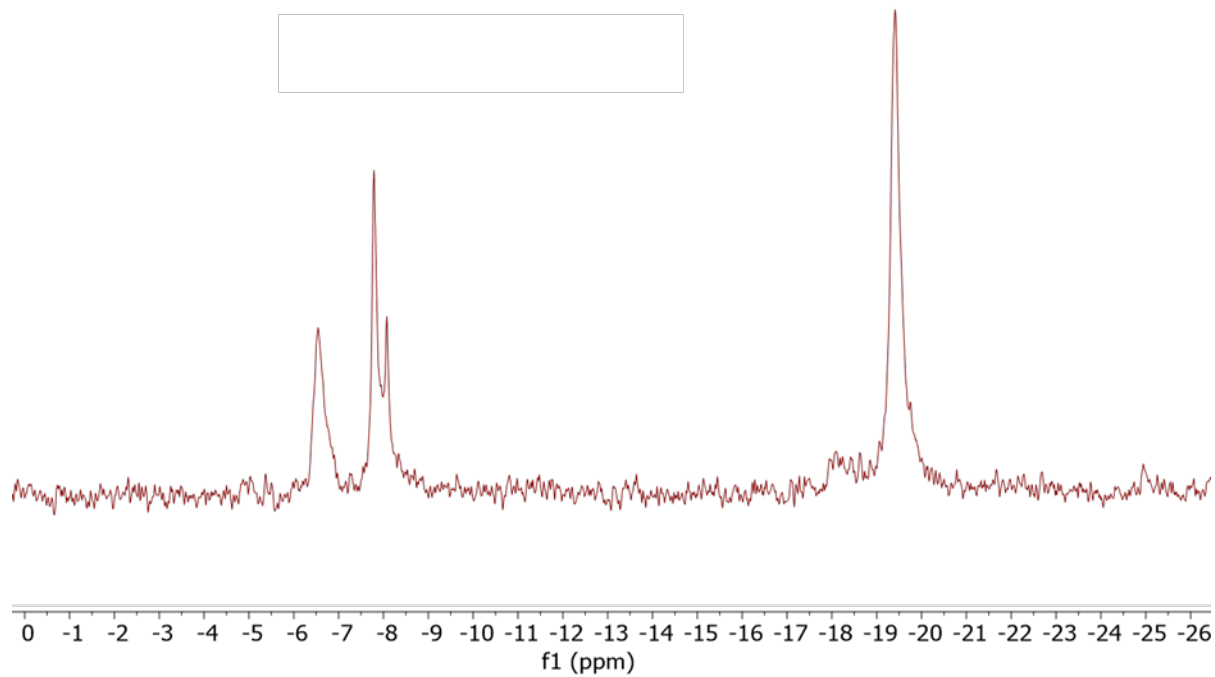


Figure S3.16 $^{31}\text{P}\{^{1}\text{H}\}$ NMR spectrum of **2et*-CCO** (temperature: -90 °C, solvent: C_7D_8)

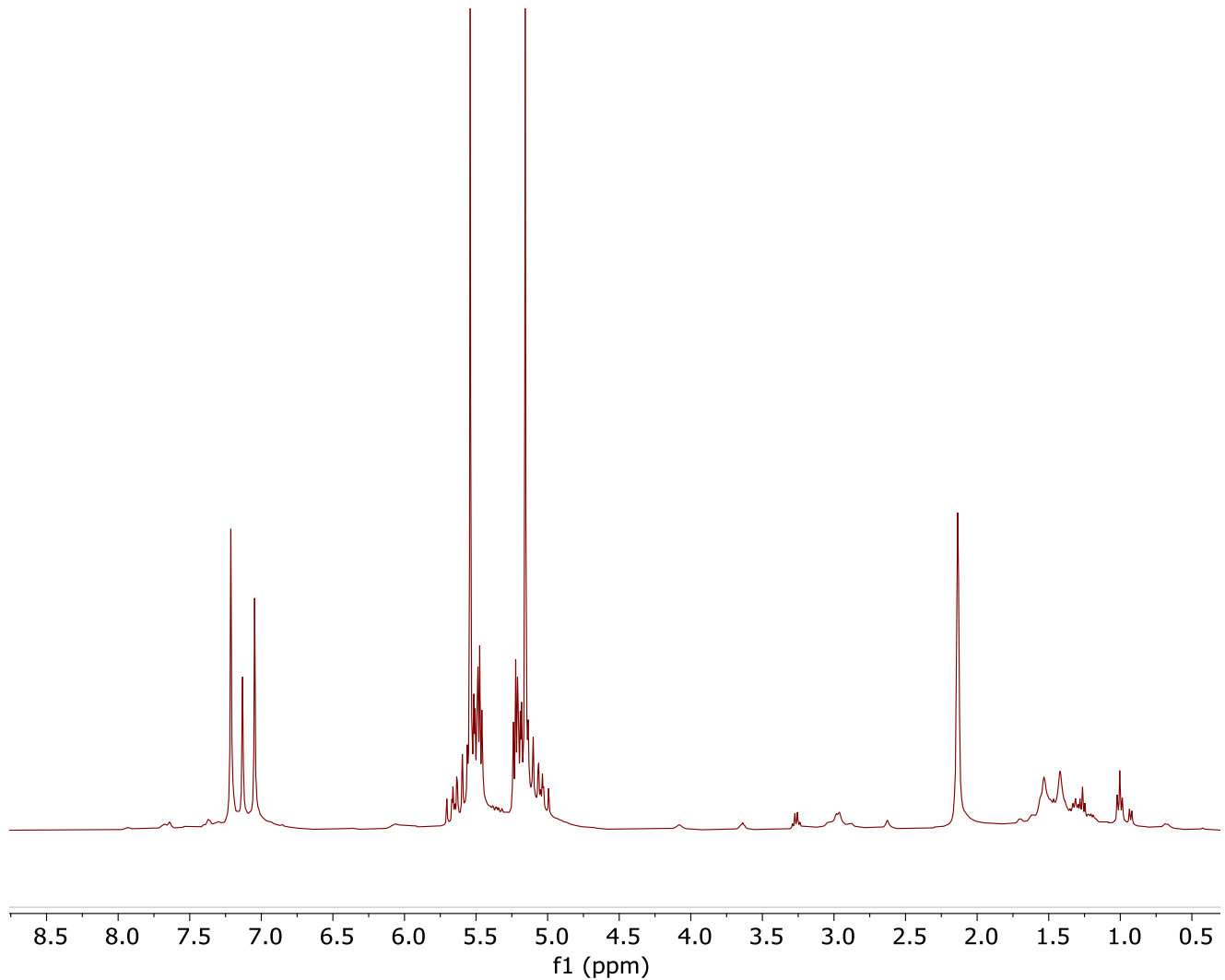


Figure S3.17 ¹H NMR spectrum of **2et*-CCO** in the presence of 4 atm. ethylene

(temperature: -90 °C, solvent: C₇D₈)

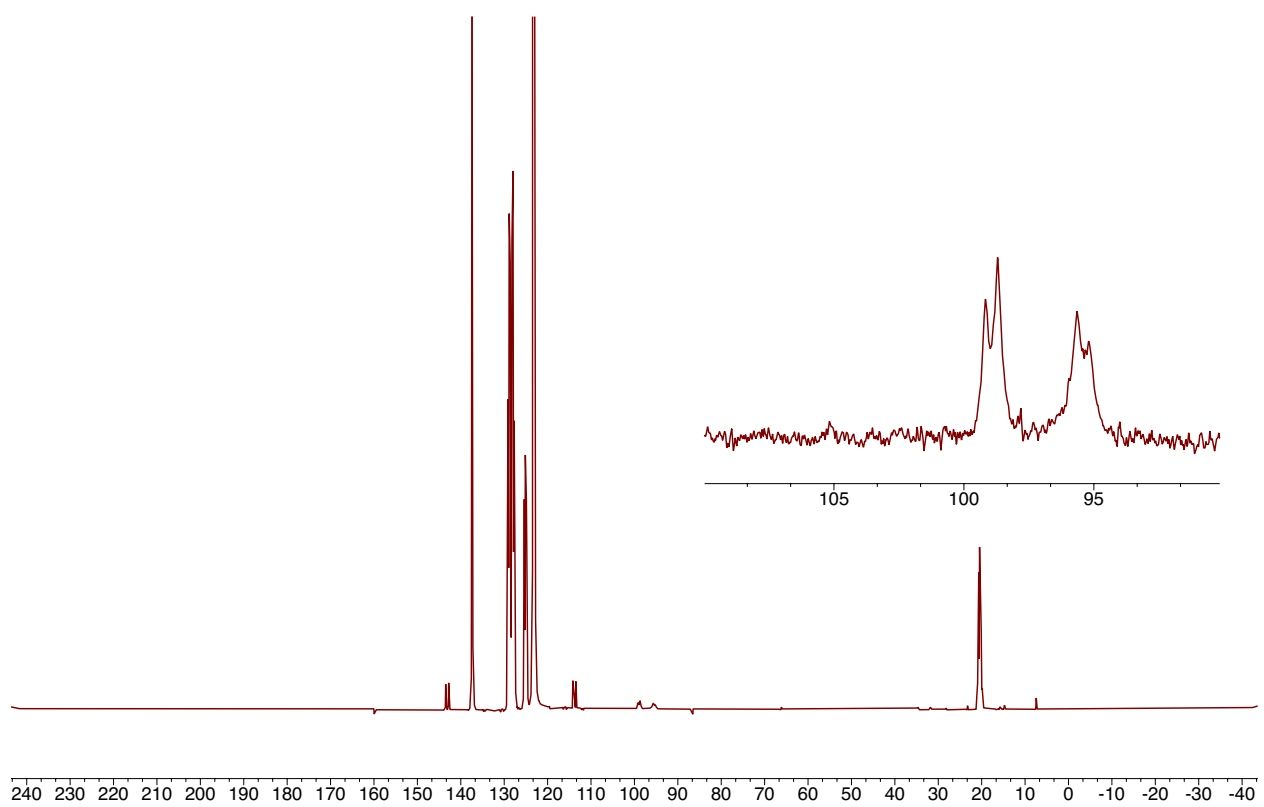


Figure S3.18 $^{13}\text{C}\{\text{H}\}$ NMR spectrum of 2^{13}et-CCO in the presence of 4 atm. ethylene
(temperature: -90 °C, solvent: C_7D_8)

Formation of **2py-CCO** from the addition of pyridine to a mixture of **2-CCO** and **2et-CCO**

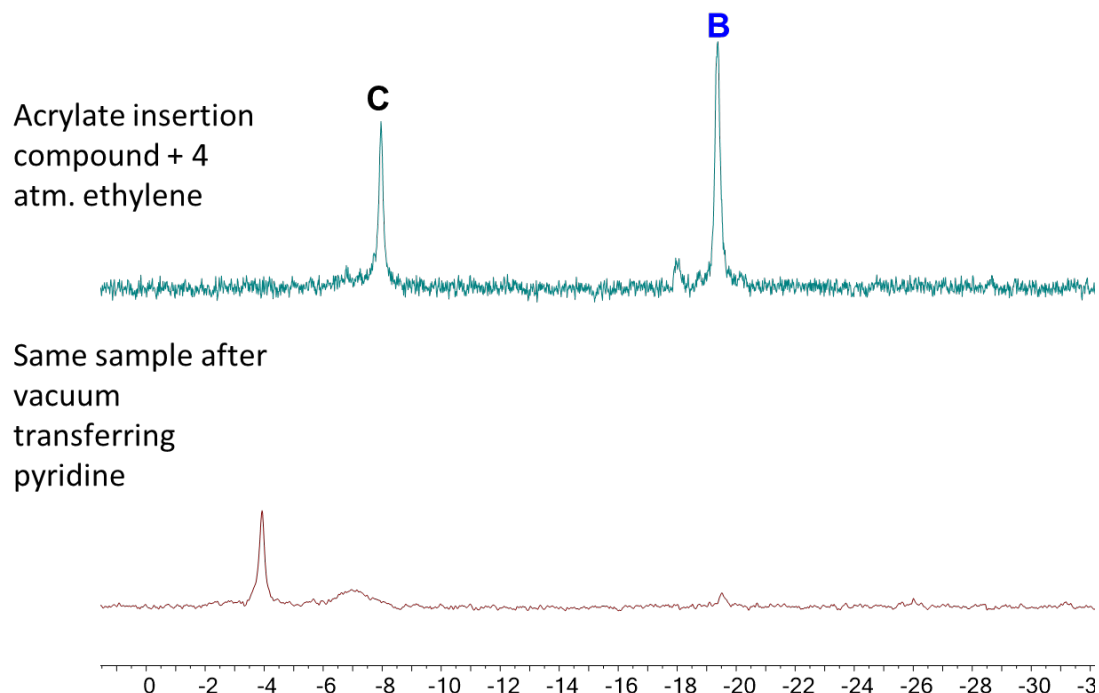


Figure S3.19 $^{31}\text{P}\{\text{H}\}$ NMR spectra of (top) **2-CCO** (acrylate insertion compound, C) + **2et-CCO** (B) and (bottom) **2-CCO** + **2et-CCO** + **2py-CCO**. (Temperature: -90 °C, solvent: C_7D_8)

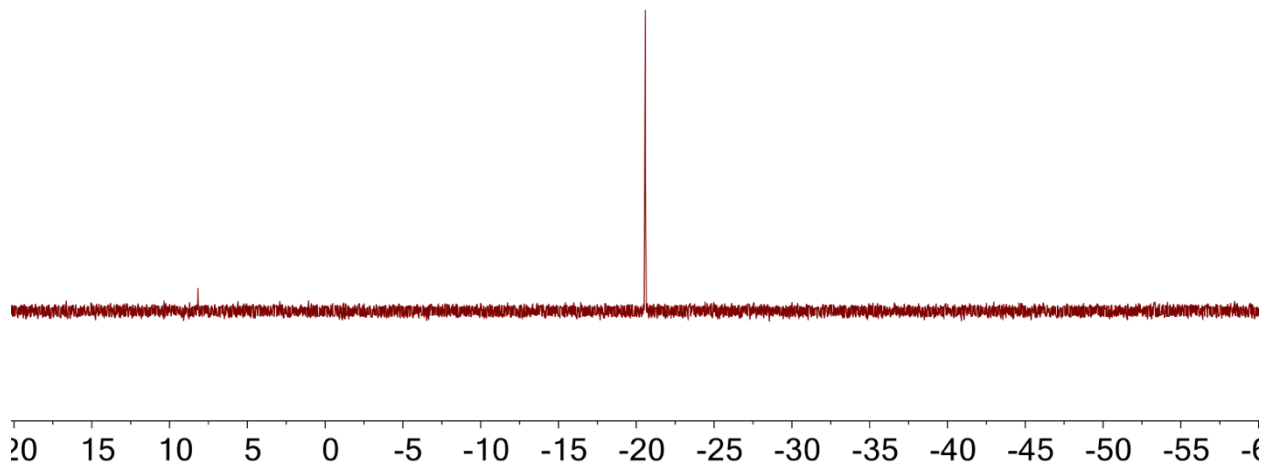


Figure S3.20 $^{31}\text{P}\{\text{H}\}$ NMR spectra of **2-C₈H₁₃** (temperature: 25 °C, solvent: C₆D₆)

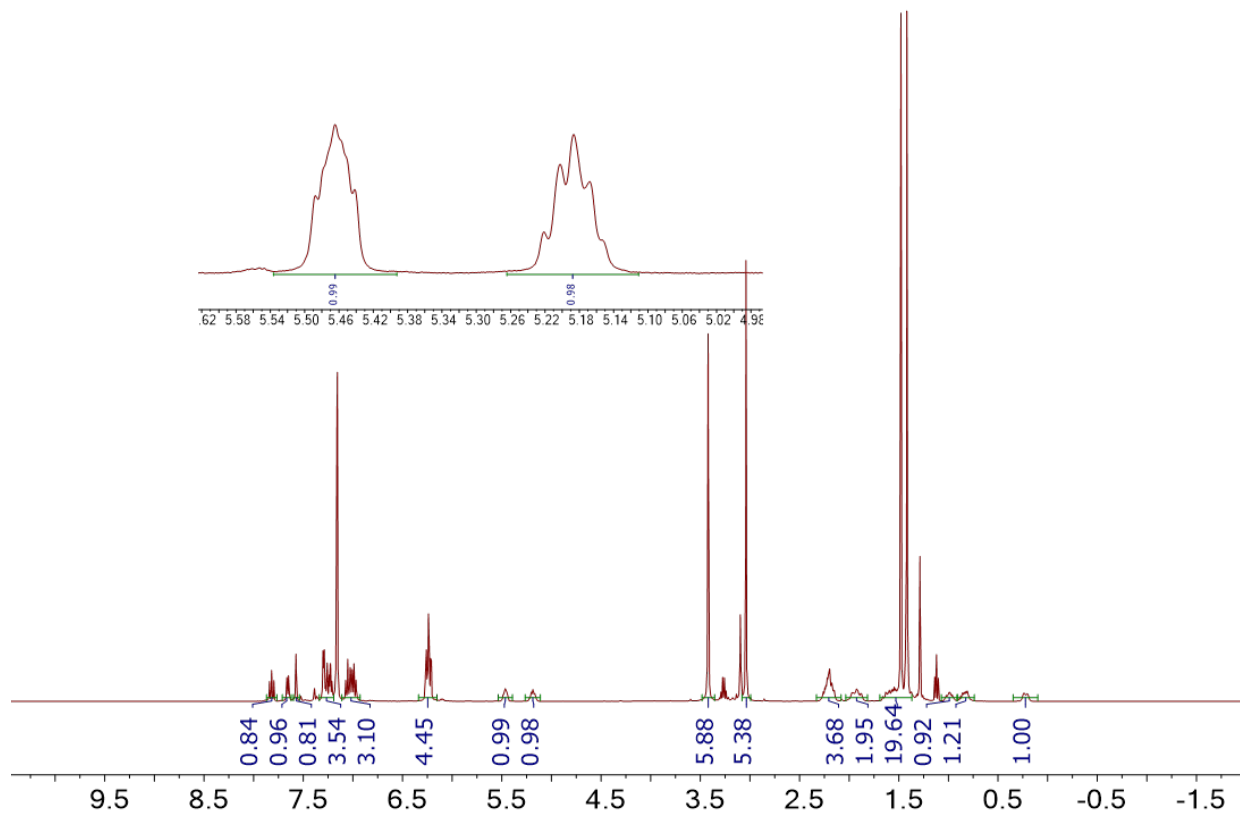


Figure S3.21 ^1H NMR spectra of **2-C₈H₁₃** (temperature: 25 °C, solvent: C₆D₆)

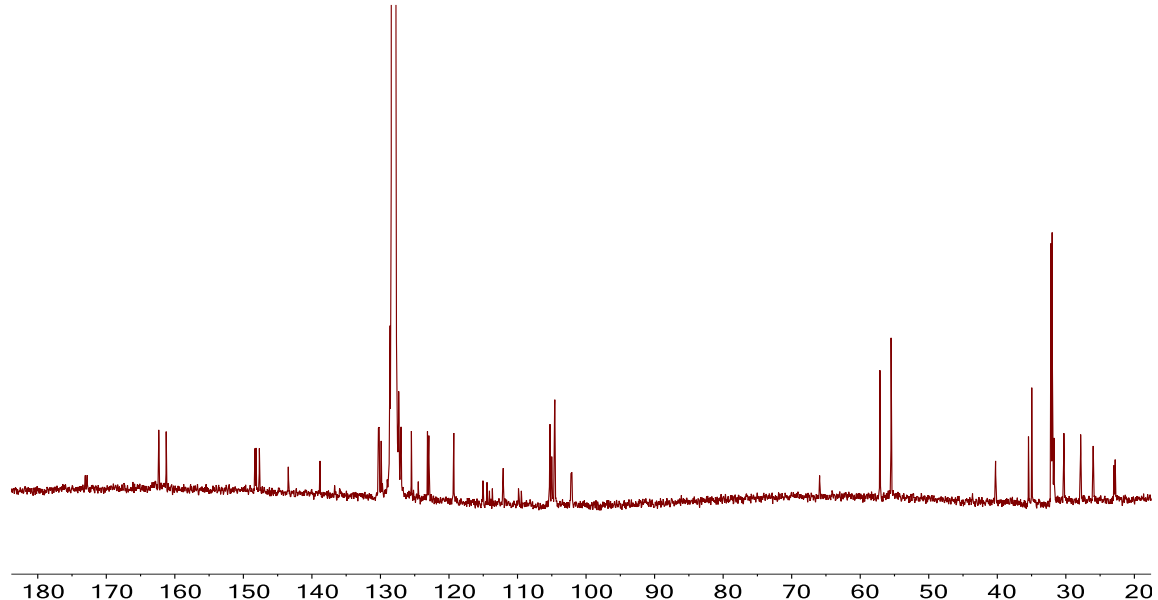


Figure S3.22 $^{13}\text{C}\{\text{H}\}$ NMR spectra of **2-C₈H₁₃** (temperature: 25 °C, solvent: C₆D₆)

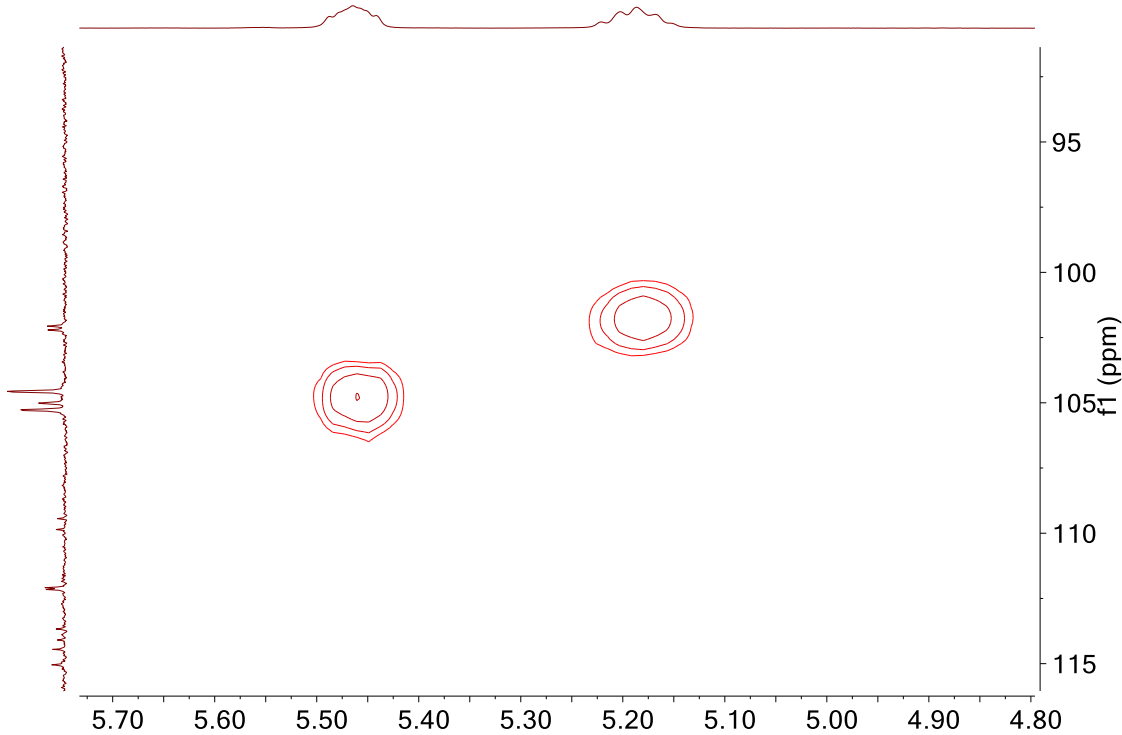


Figure S3.23 $^{13}\text{C}\{\text{H}\}$ - ^1H HSQC NMR Spectrum of **2-C₈H₁₃** (temperature: 25 °C, solvent: C₆D₆)

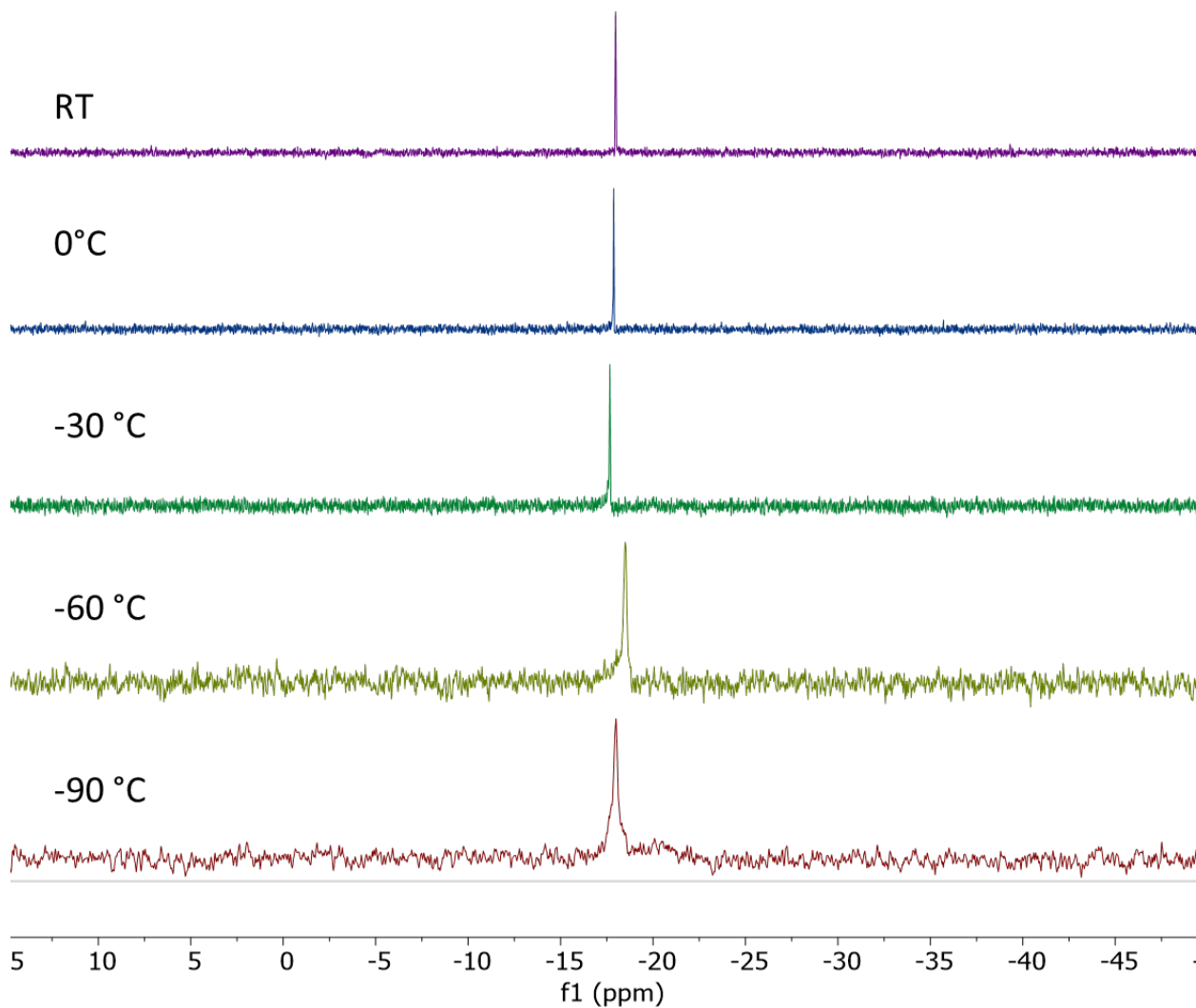


Figure S3.24 $^{31}\text{P}\{\text{H}\}$ NMR Spectra of **2-C₈H₁₃** at different temperatures (solvent: C₇D₈).

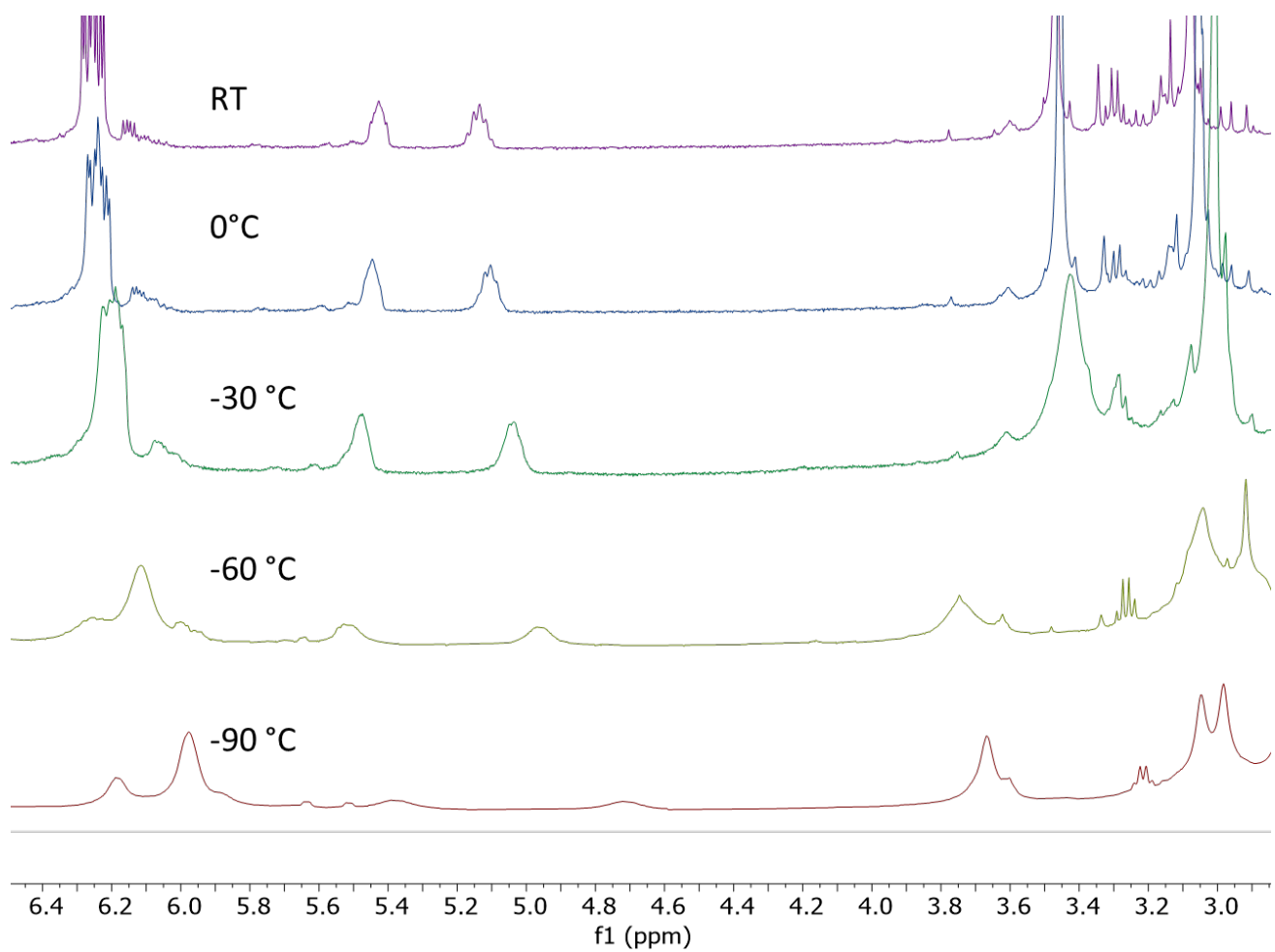


Figure S3.25 ^1H NMR Spectra of **2-C₈H₁₃** at different temperatures (Olefinic region, solvent: C₇D₈).

$^{31}\text{P}\{\text{H}\}$ NMR Spectrum of PONap-Ni-CCO + POP-Ni-CCO-Py

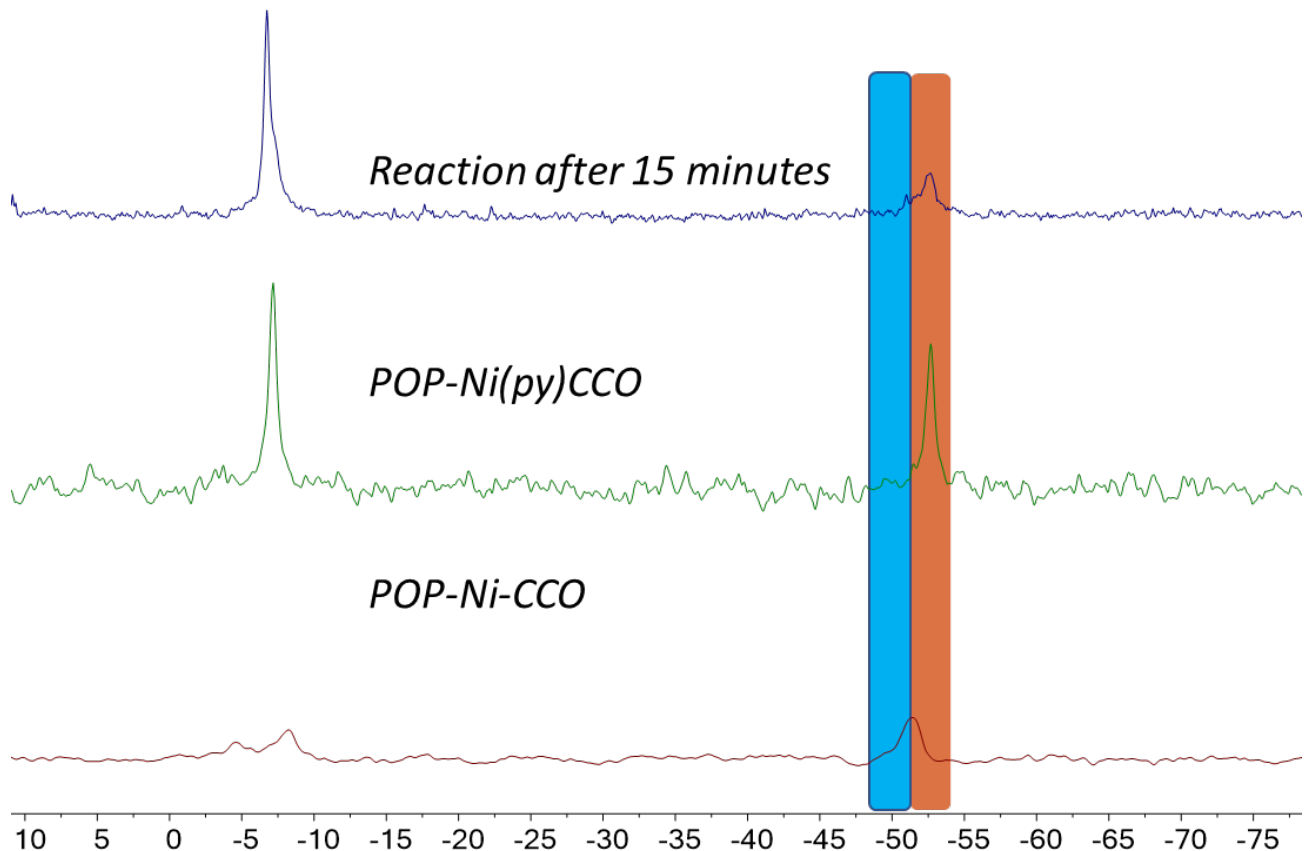


Figure S3.26 $^{31}\text{P}\{\text{H}\}$ NMR of mixture of **1py-CCO + 2-CCO** (top), **1py-CCO** (medium) and **1-CCO** (bottom) in C_6D_6

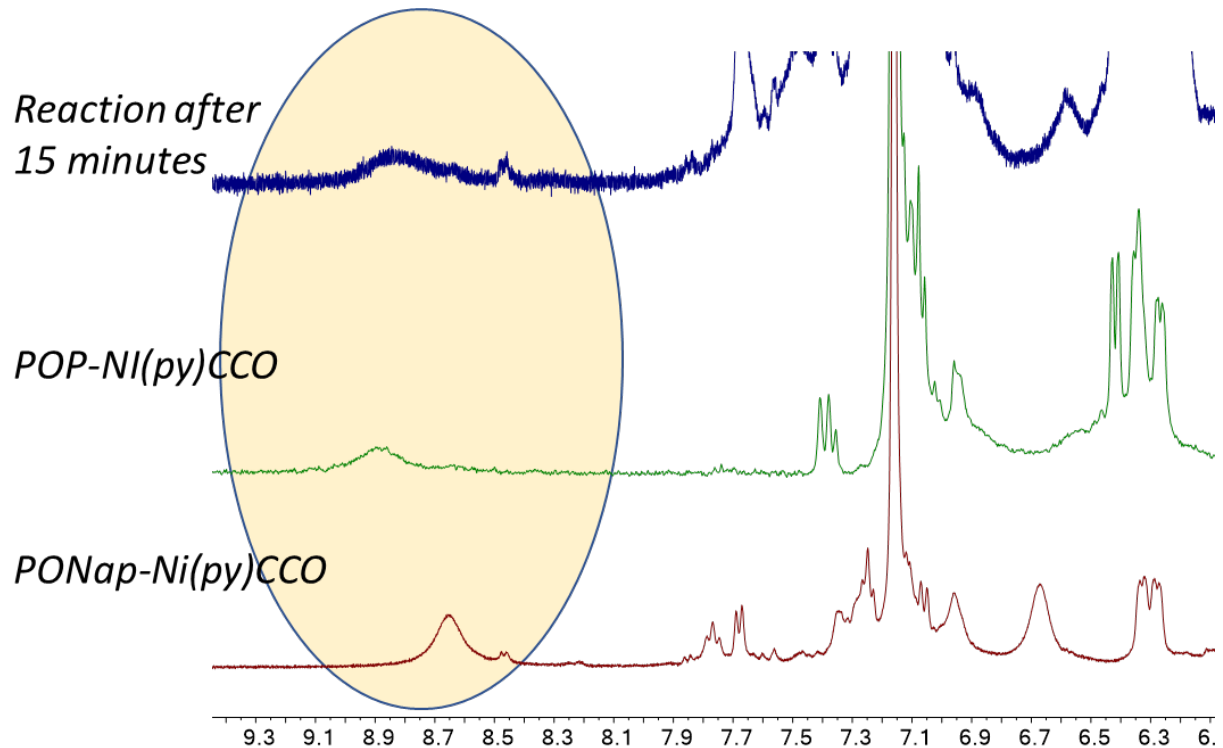


Figure S3.27 ${}^3\text{1}\text{P}\{{}^1\text{H}\}$ NMR of mixture of **1py-CCO + 2-CCO** (top), **1py-CCO** (medium) and **2-CCO** (bottom) in C_6D_6

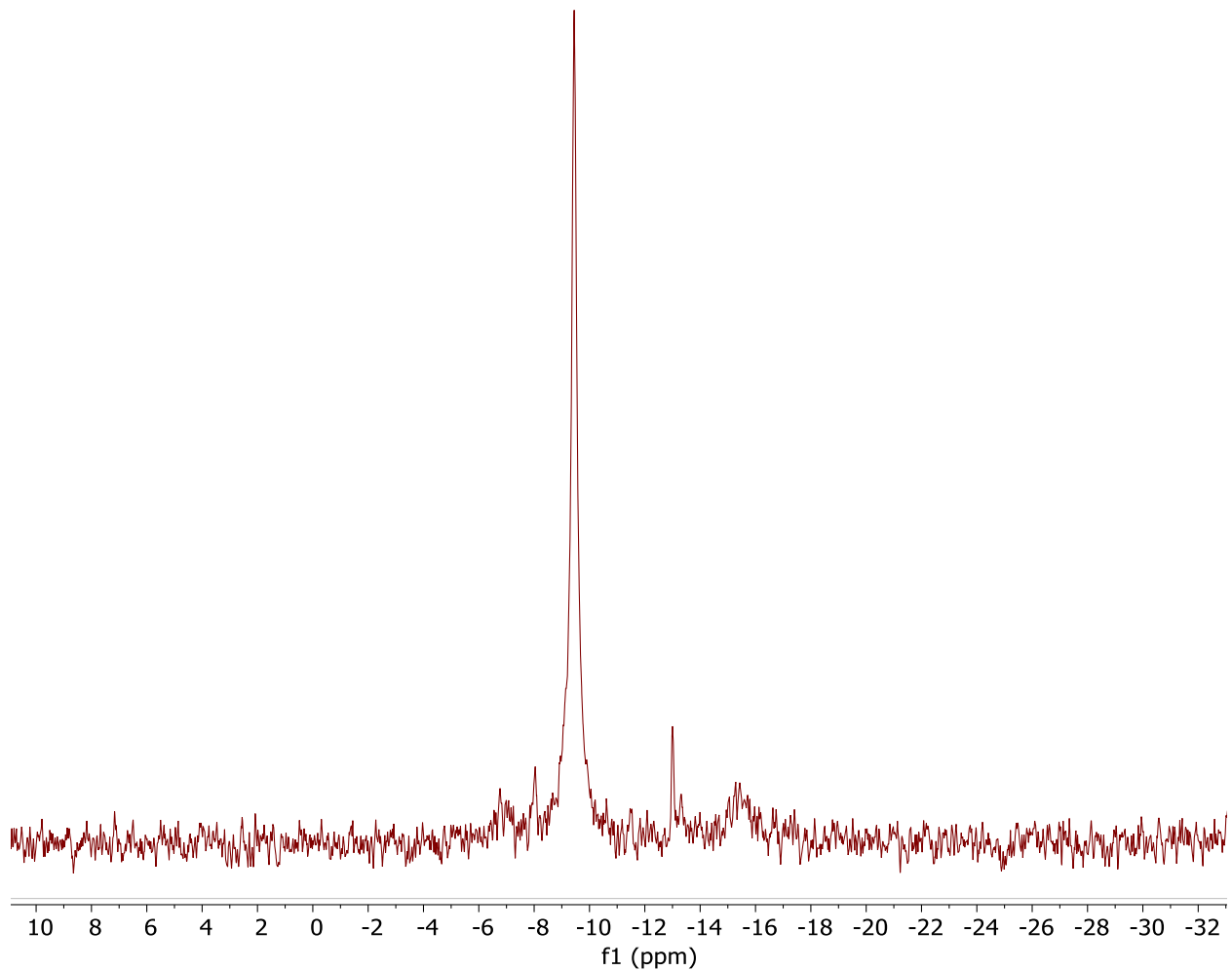


Figure S3.28 ${}^{31}\text{P}\{{}^1\text{H}\}$ NMR spectrum of mixture of **2lut-CCO** at -90 °C in tol-d_8 .

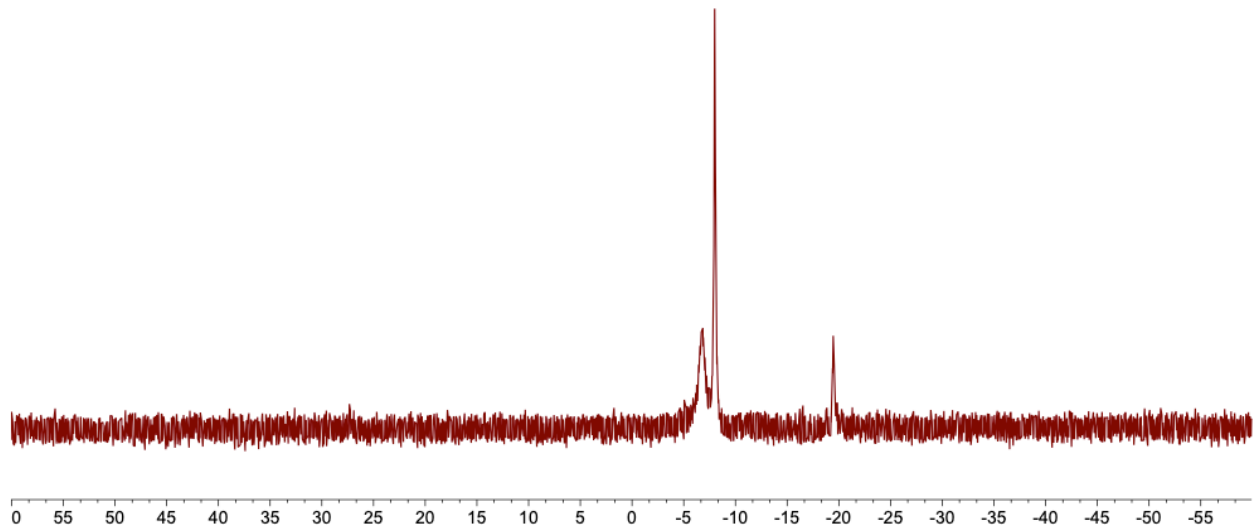


Figure S3.29 ${}^3\text{P}\{{}^1\text{H}\}$ NMR spectrum of thermodynamic mixture of **2-CCO** and **2et-CCO** at $-90\text{ }^\circ\text{C}$ in tol-d8 .

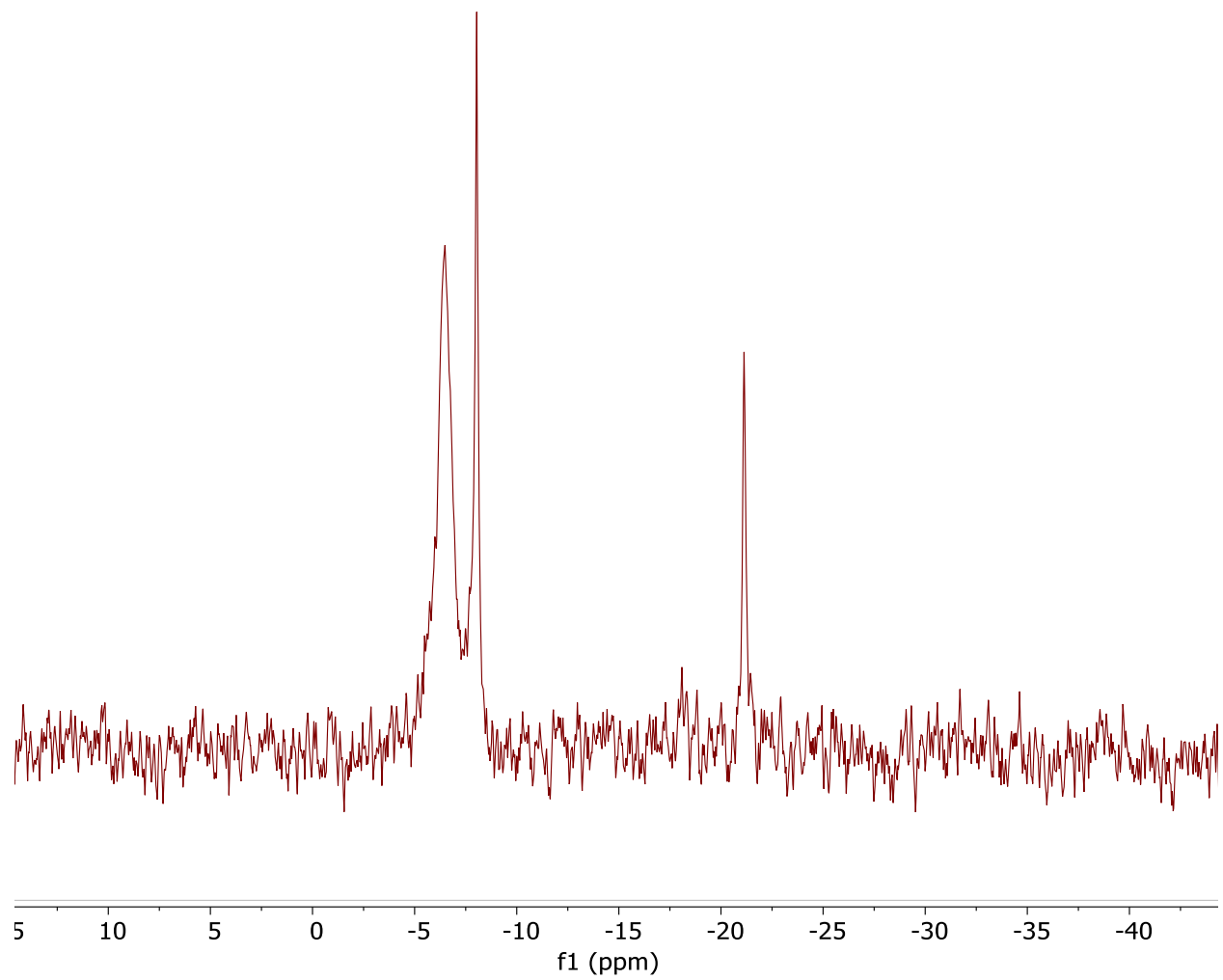


Figure S3.30. ${}^3\text{1}\text{P}\{{}^1\text{H}\}$ NMR spectrum of thermodynamic mixture of **2-CCO** and **2hex-CCO** at $-90\text{ }^\circ\text{C}$ in tol-d8 .

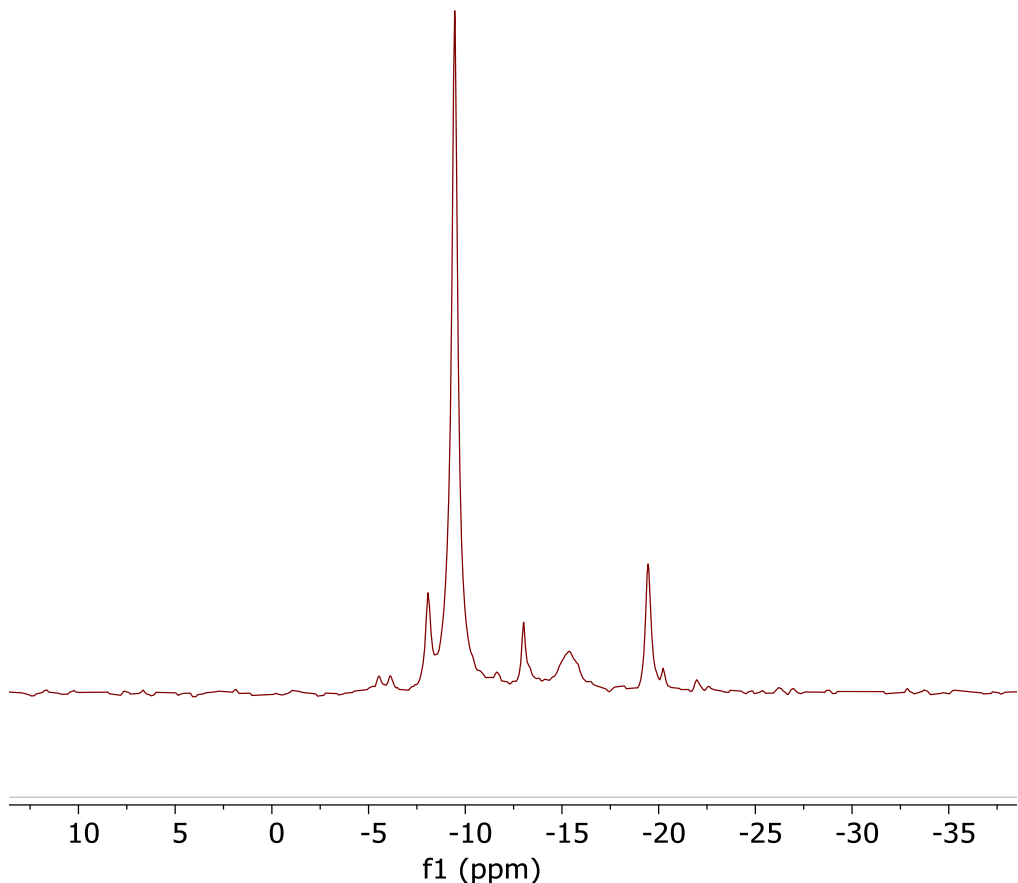


Figure S3.31. ${}^3\text{P}\{{}^1\text{H}\}$ NMR spectrum of thermodynamic mixture of **2et-CCO** and **2lut-CCO** at -90 °C in tol-d8.

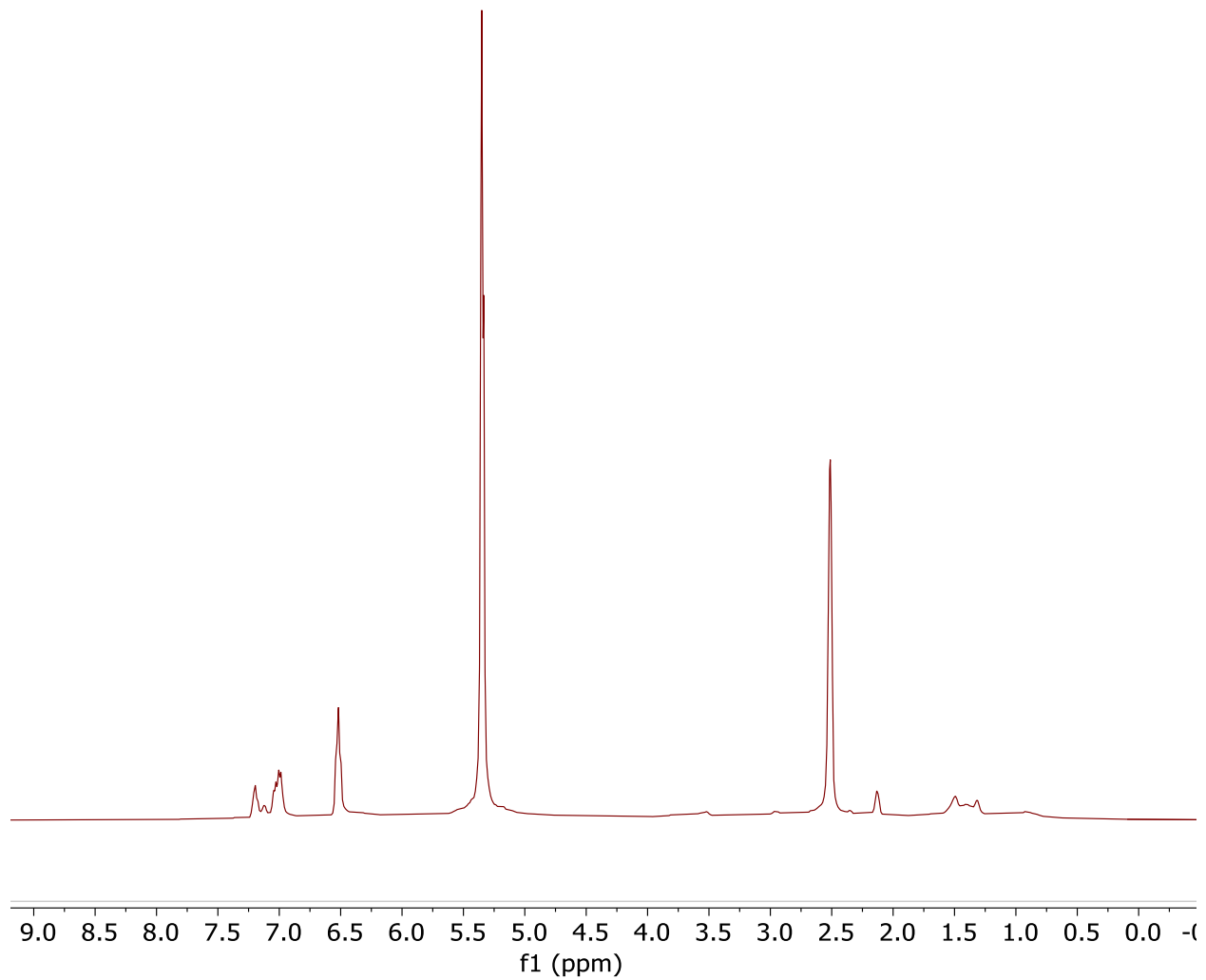


Figure S3.32. ¹H NMR spectrum of thermodynamic mixture of **2-CCO** and **2et-CCO** at -90 °C in tol-d8.

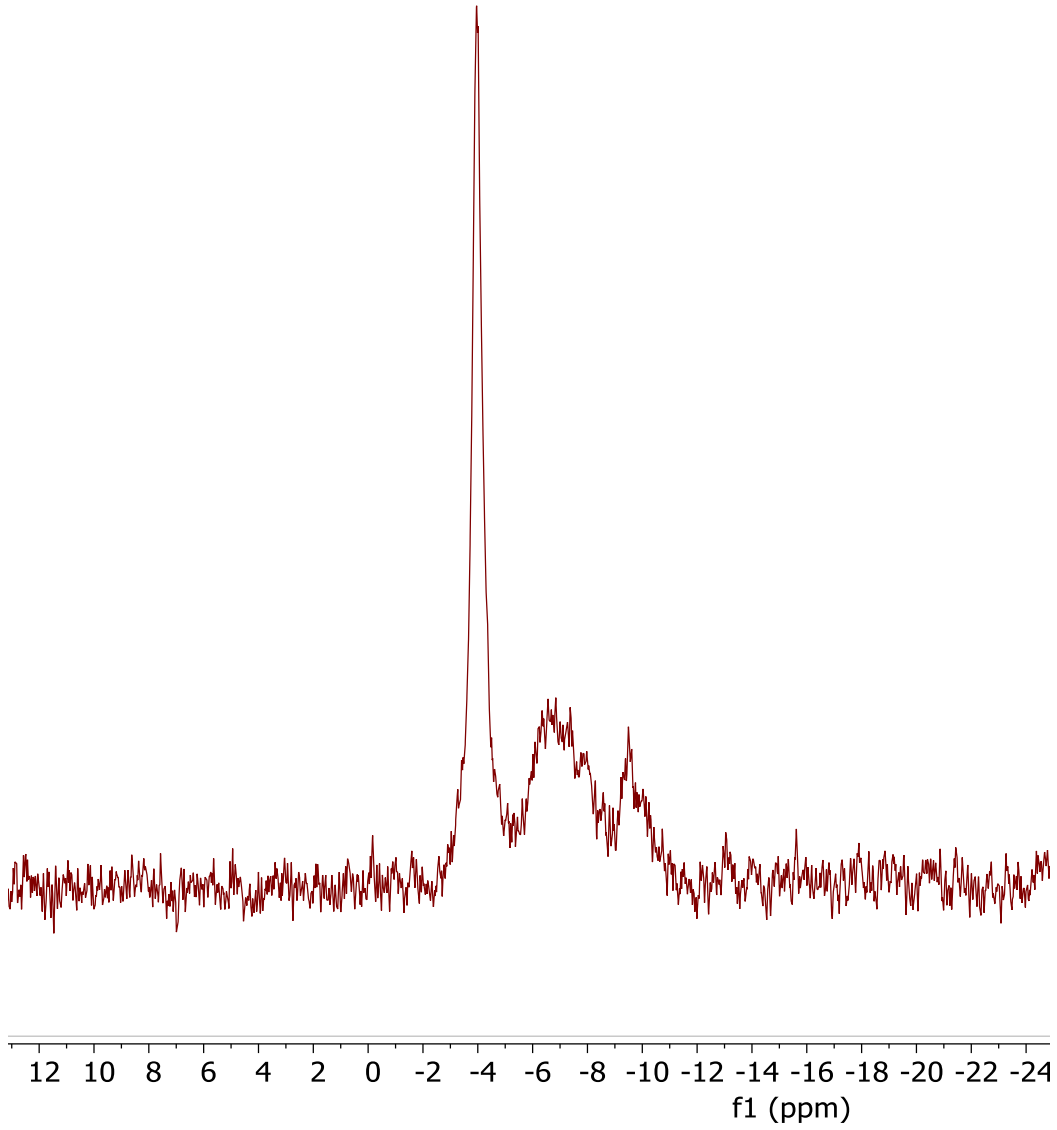


Figure S3.33. ${}^3\text{P}\{{}^1\text{H}\}$ NMR spectrum of thermodynamic mixture of **2py-CCO** and **2lut-CCO** at -90 °C in tol-d8.

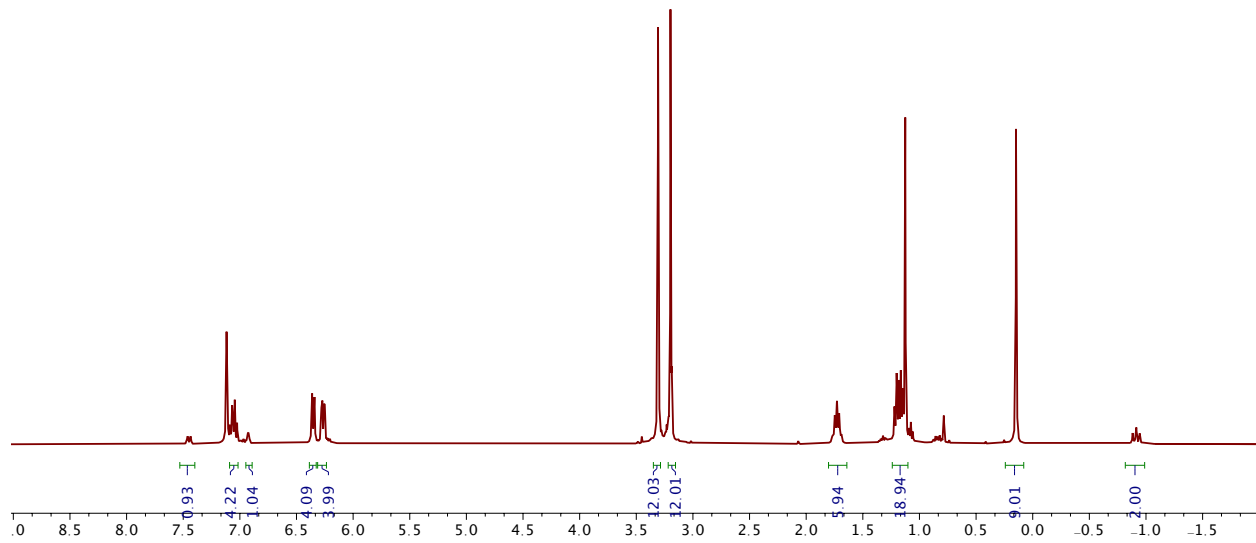


Figure S3.34. ^1H NMR spectrum of **1P** in C_6D_6 .

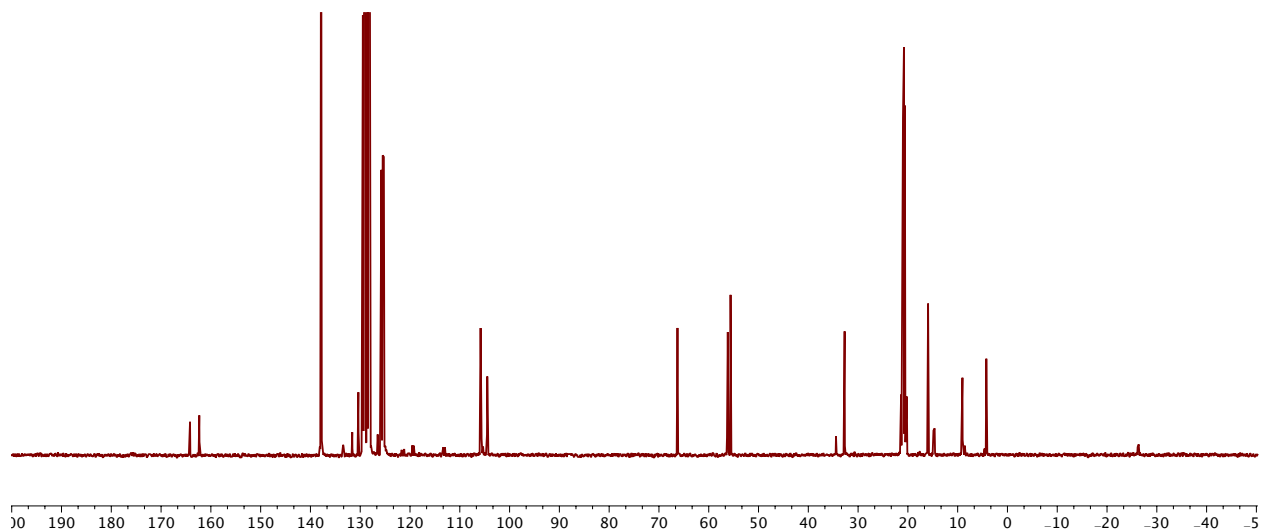


Figure S3.35. $^{13}\text{C}\{^1\text{H}\}$ NMR spectrum of **1P** in tol-d_8 .

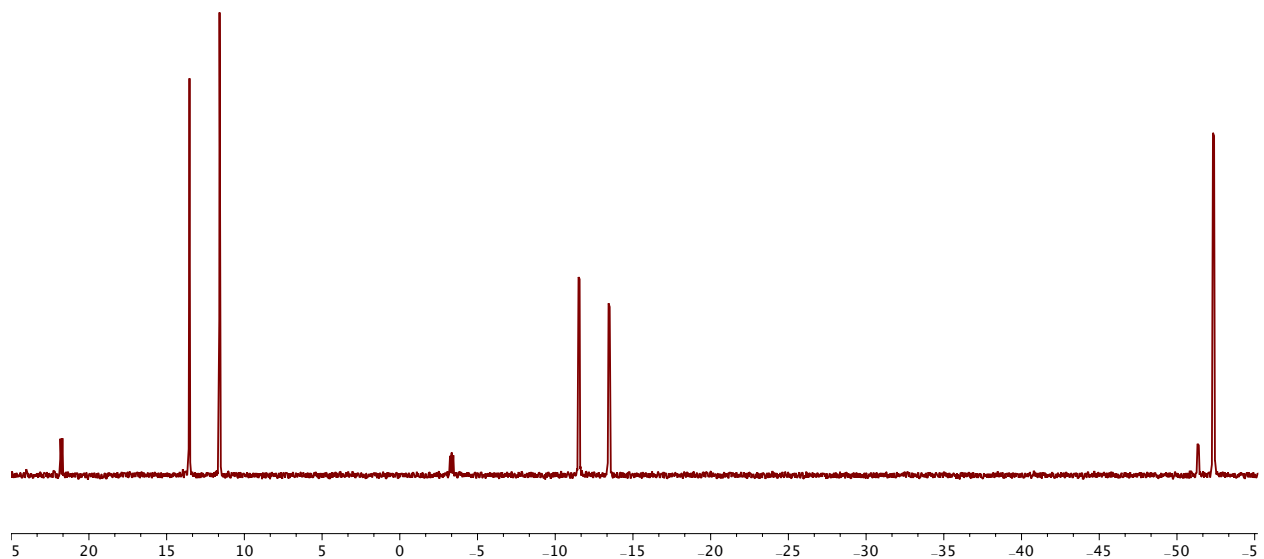


Figure S3.36. ${}^{31}\text{P}\{{}^1\text{H}\}$ NMR spectrum of **1P** in tol-d_8 .

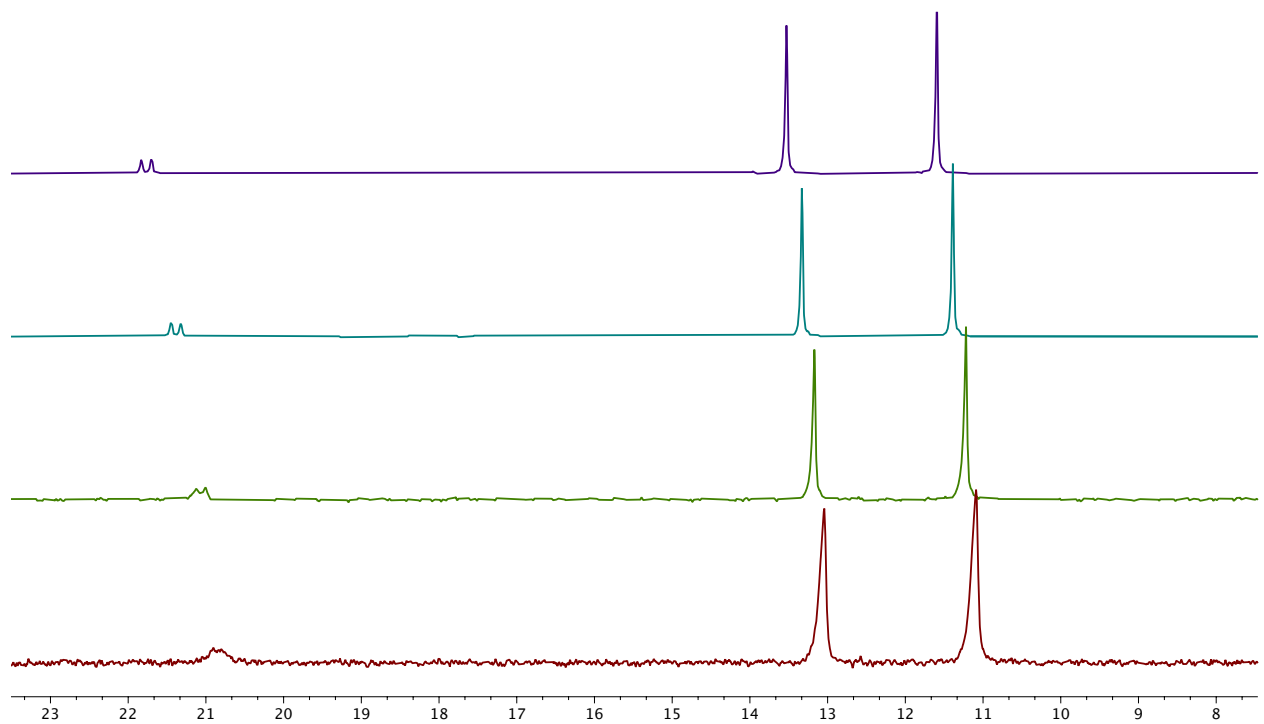


Figure S3.37. ${}^{31}\text{P}\{{}^1\text{H}\}$ NMR spectrum of **1P** in tol-d_8 at different temperatures (top to bottom: 25 °C, 50 °C, 70 °C, 90 °C)

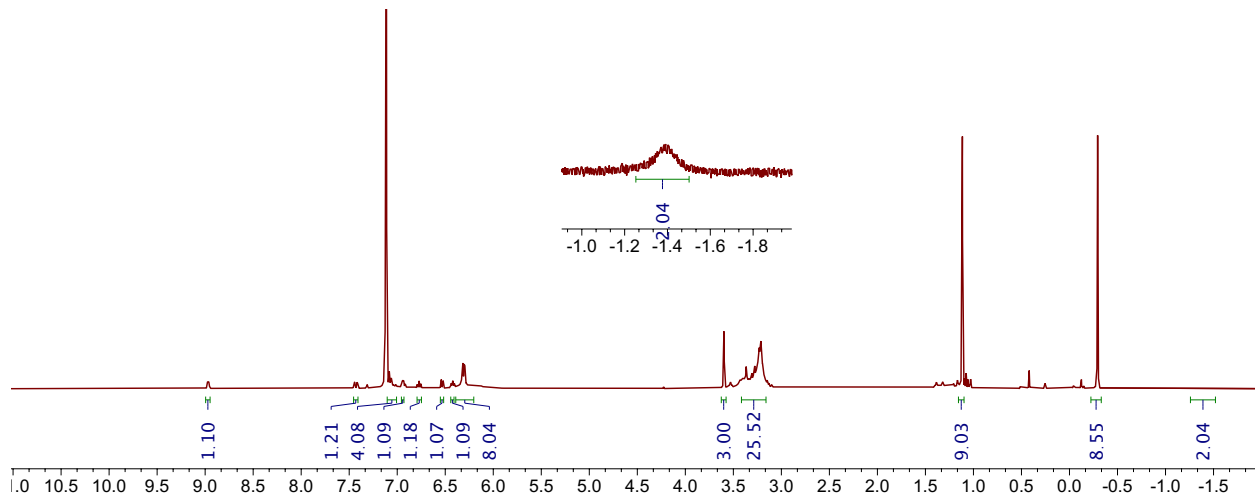


Figure S3.38. ^1H NMR spectrum of **1pico** in C_6D_6 .

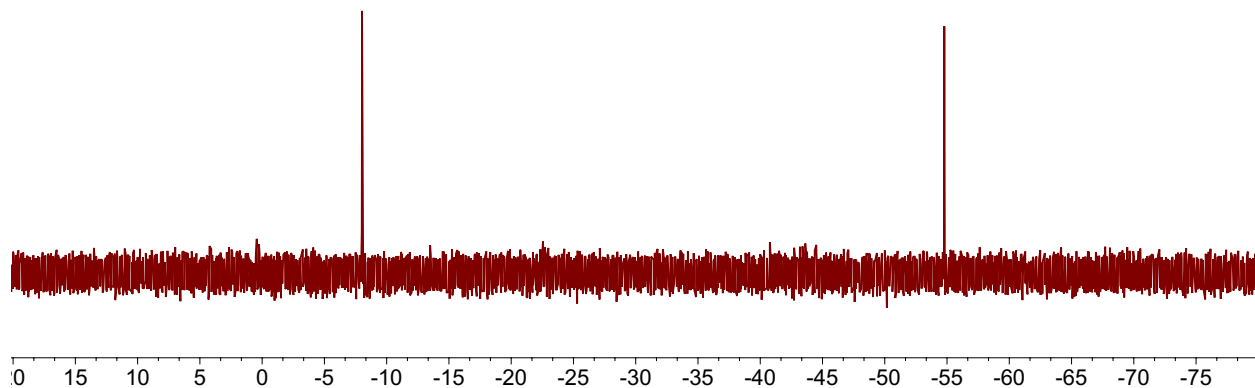


Figure S3.39. $^{31}\text{P}\{^1\text{H}\}$ NMR spectrum of **1pico** in C_6D_6 .

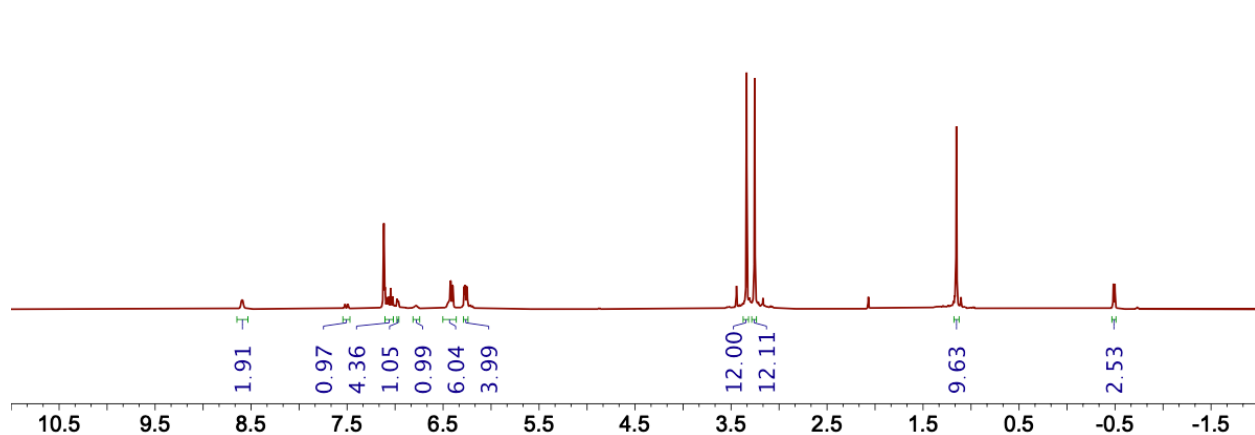


Figure S3.40. ^1H NMR spectrum of **1py-Me** in C_6D_6 .

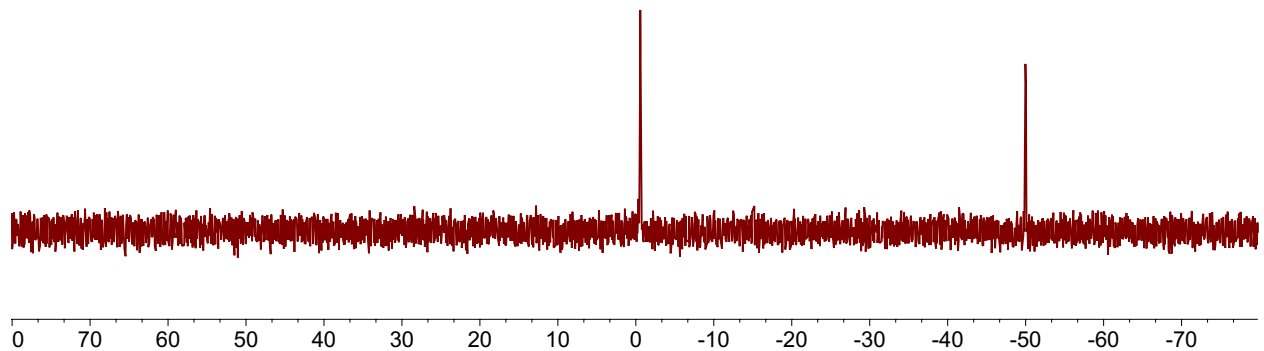


Figure S3.41. $^{31}\text{P}\{\text{H}\}$ NMR spectrum of **1py-Me** in C_6D_6 .

4. Quantitative Determination of Ligand Binding Strengths

Determination of Thermodynamic Binding Constants with substituted pyridines:

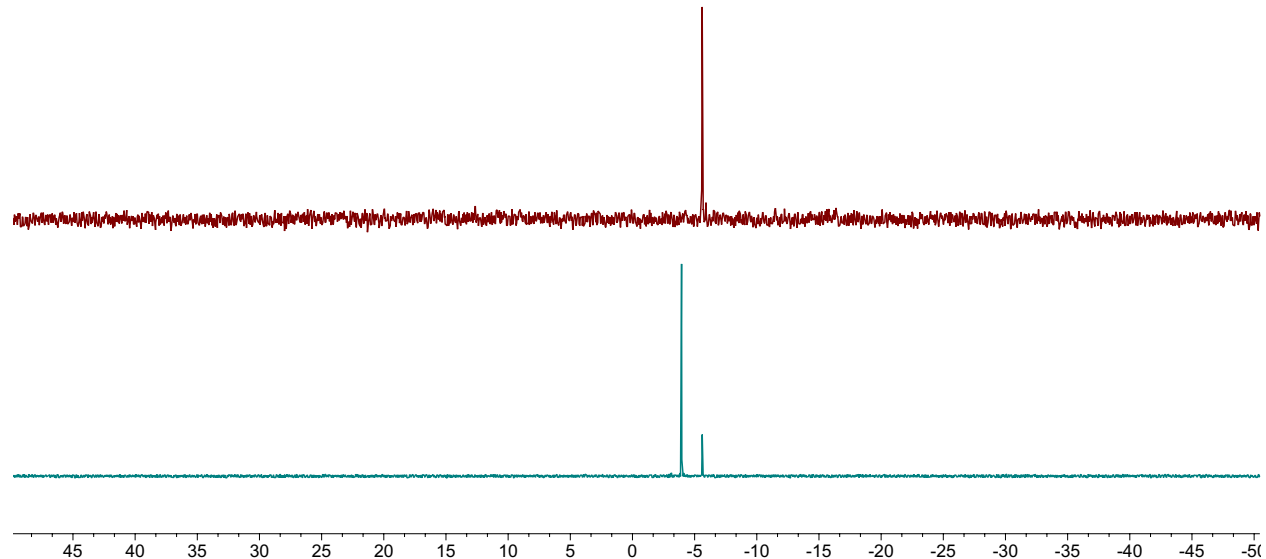


Figure S4.1. An example of the determination of K value via $^{31}\text{P}\{^1\text{H}\}$ NMR spectra (method 1): (Top) $^{31}\text{P}\{^1\text{H}\}$ NMR spectrum of **2lut-Me** and (bottom) $^{31}\text{P}\{^1\text{H}\}$ NMR spectrum of **2lut-Me + 1 equiv. of lutidine**.

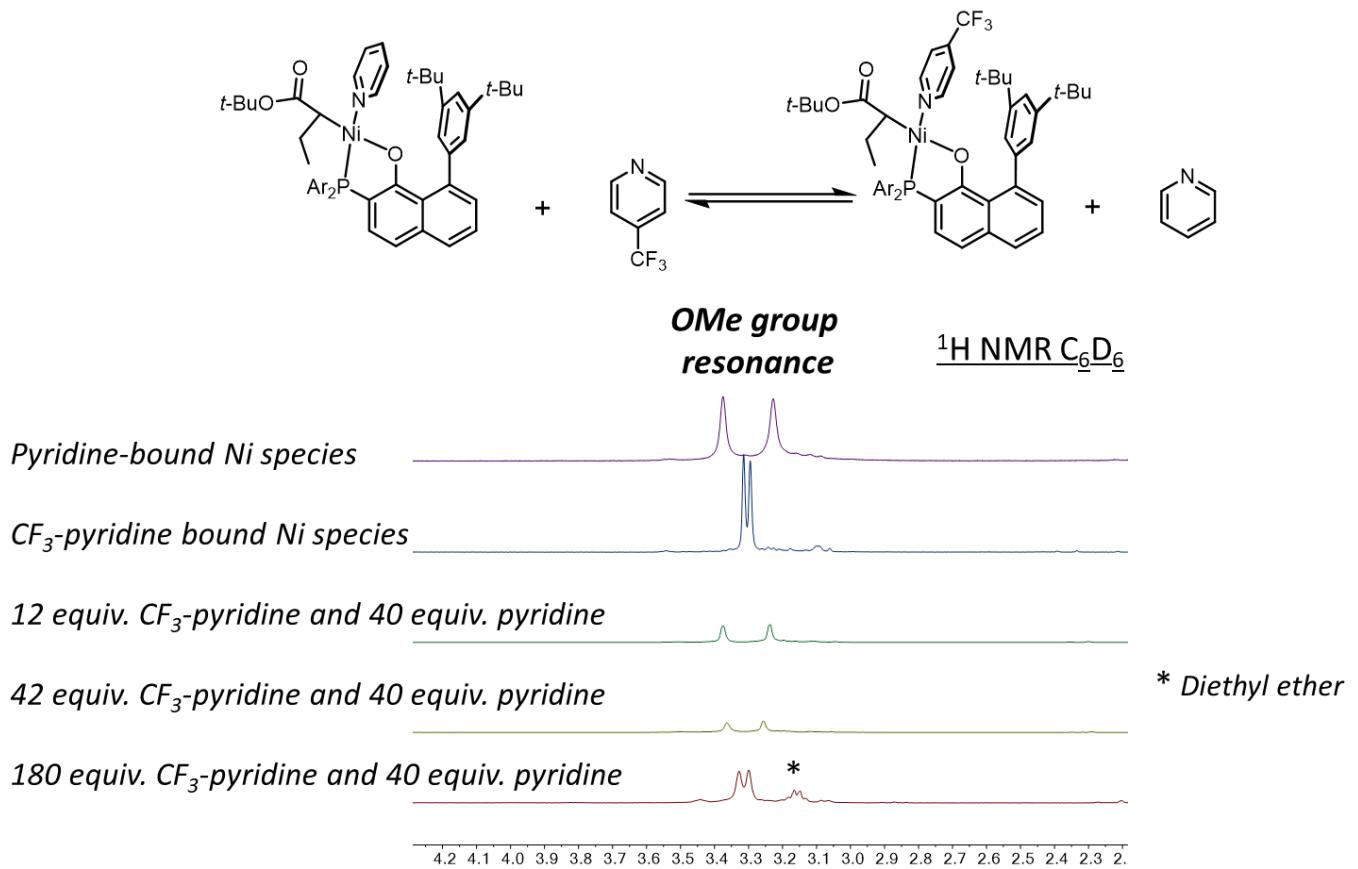


Figure S4.2. An example of the determination of K value via ^1H NMR spectra (method 2).

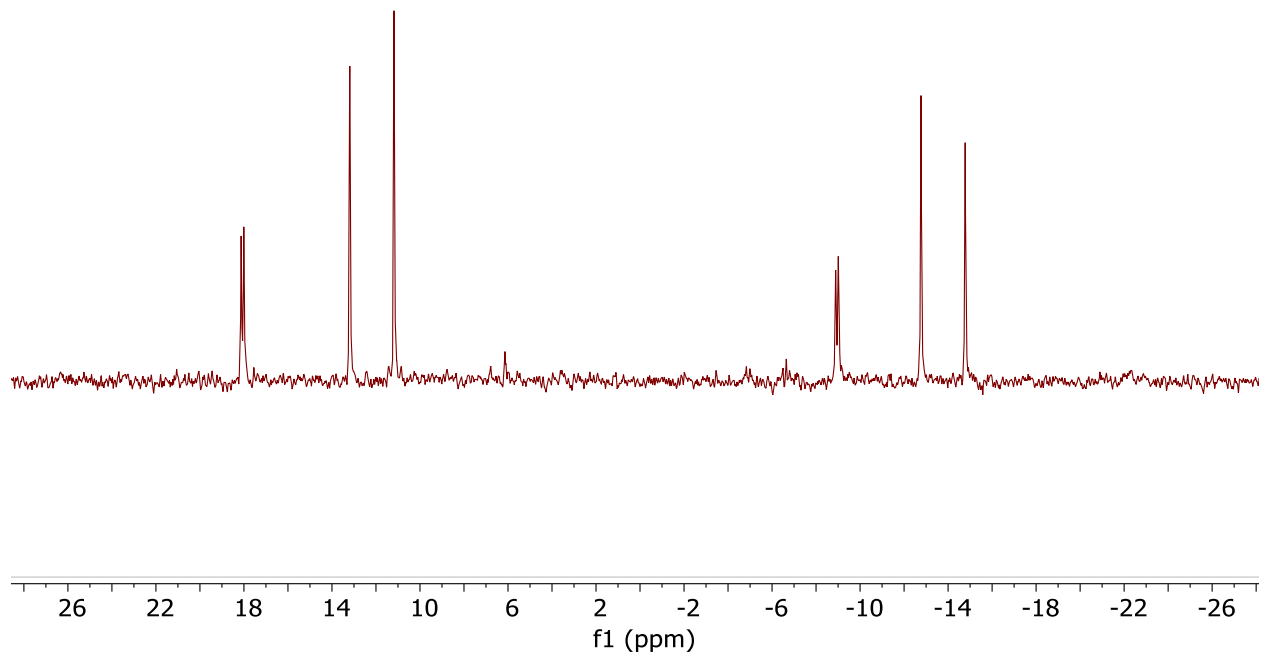


Figure S4.3. $^{31}\text{P}\{\text{H}\}$ NMR spectrum **2P**.

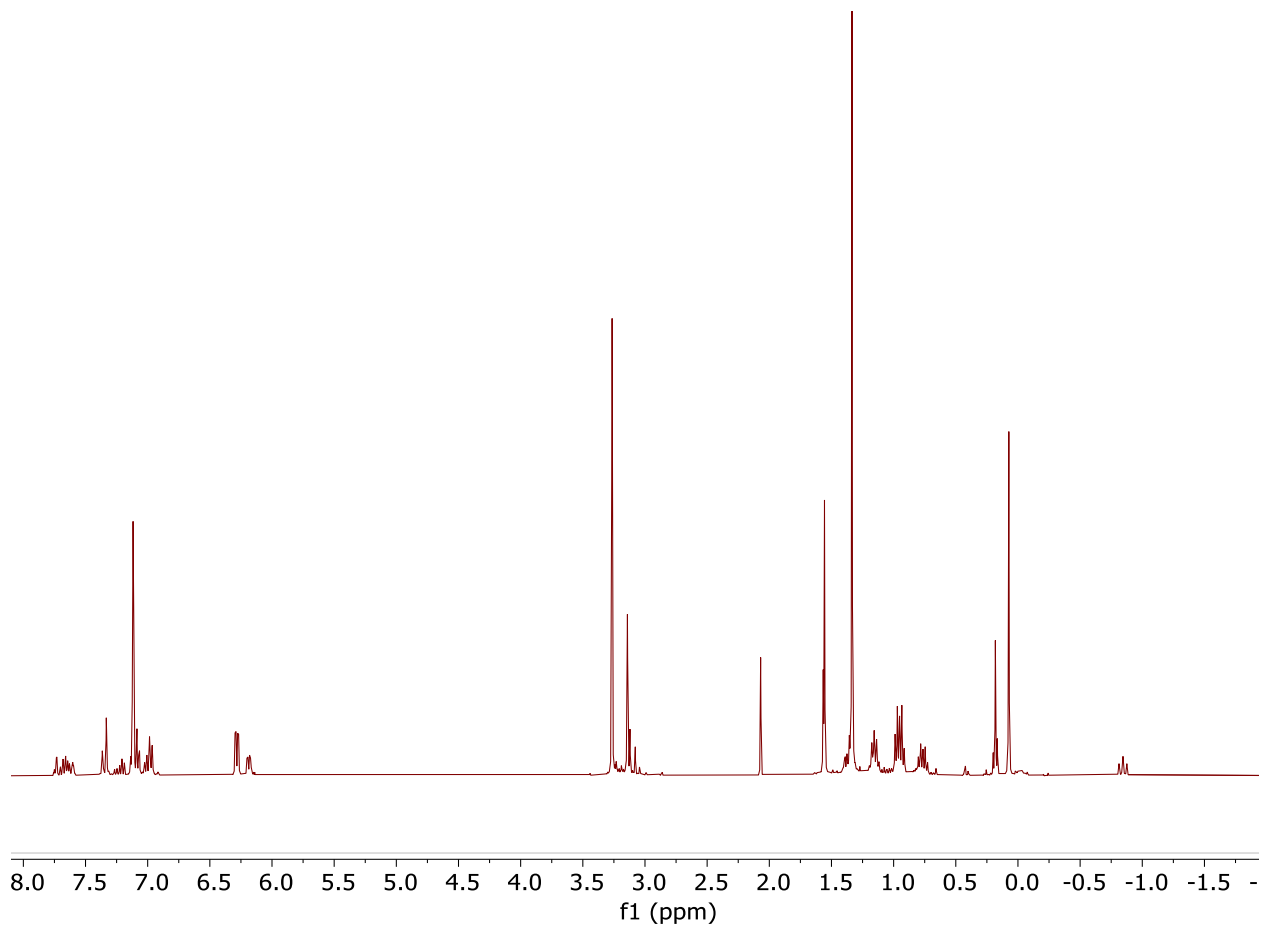
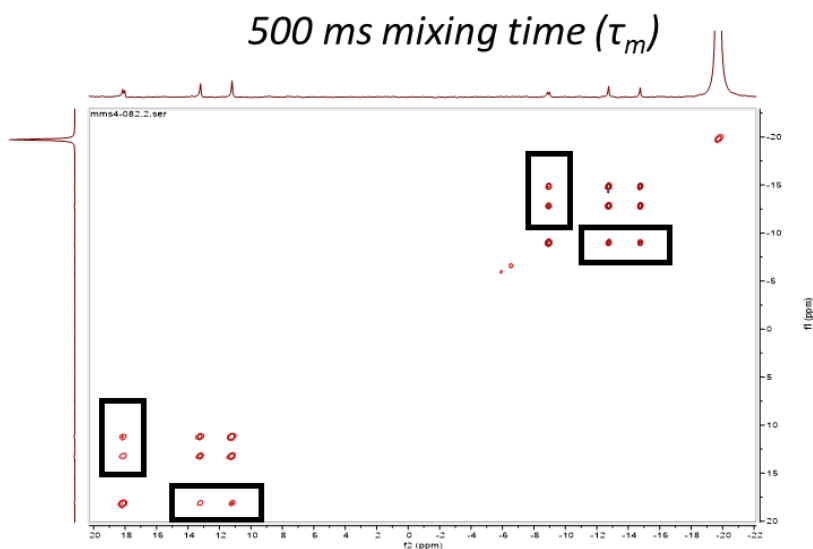
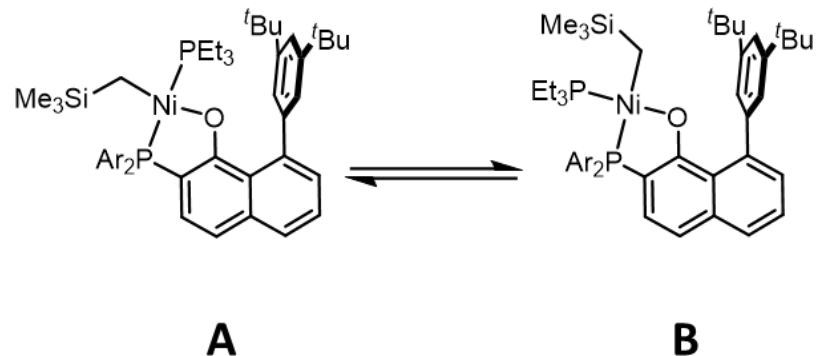
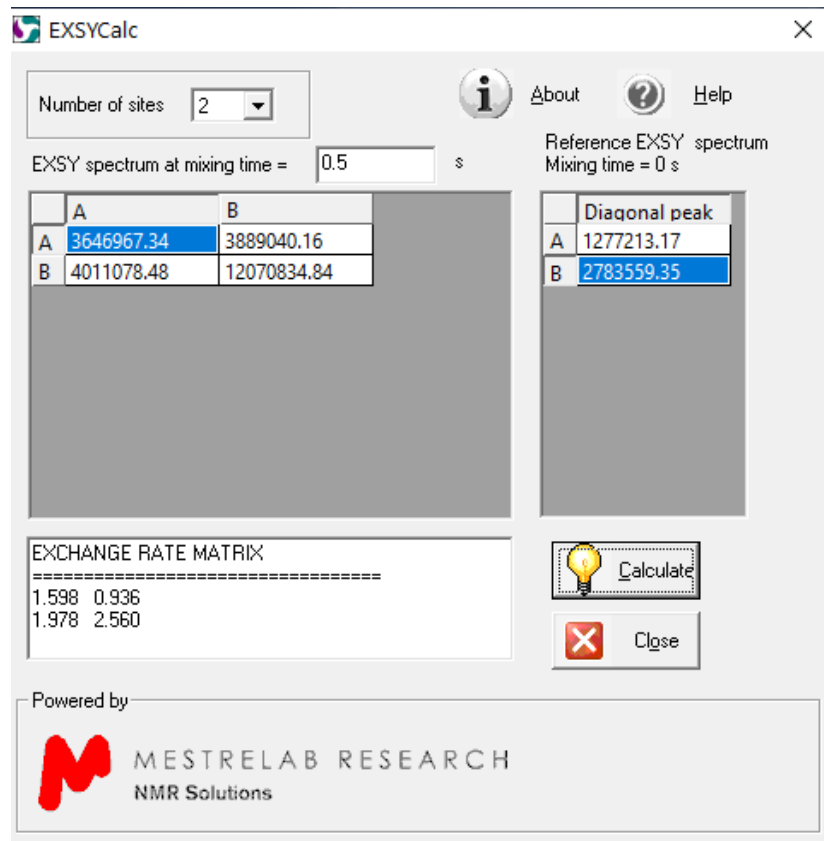
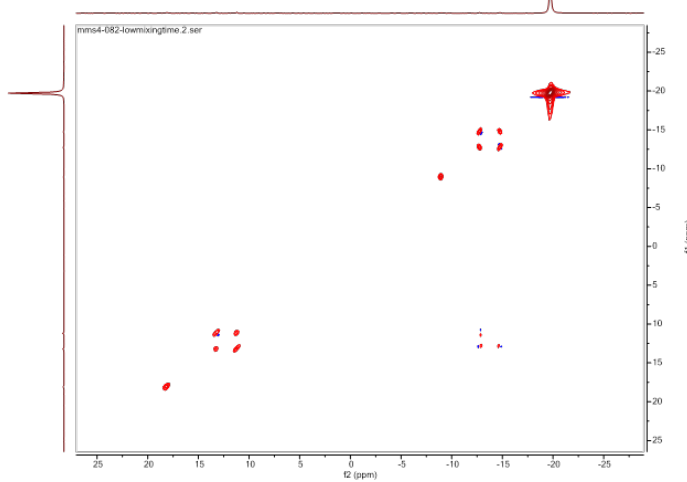


Figure S4.4. ${}^{31}\text{P}\{{}^1\text{H}\}$ NMR spectrum **2P**.

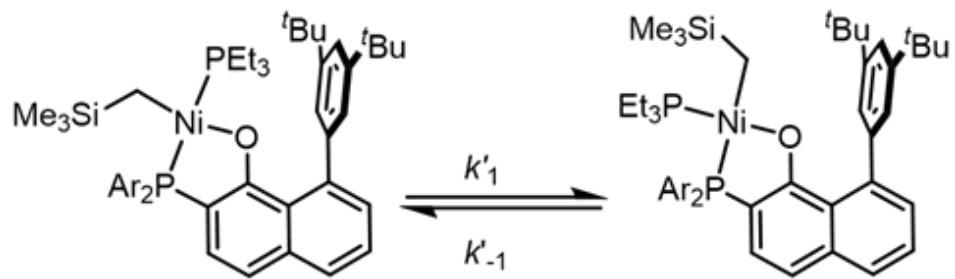
Sample of $^{31}\text{P}\{\text{H}\}$ EXSY Experiment of 2P



3 ms mixing time (τ_m)



X equiv. PEt₃



X	k'_1	k'_{-1}
0	0.6 s ⁻¹	1.8 s ⁻¹
10	0.9 s ⁻¹	2.0 s ⁻¹
40	0.9 s ⁻¹	1.9 s ⁻¹

5. Supplemental information for olefin copolymerization

5.1 Procedures for polymerization and polymer characterization

5.1.1 General procedure for high throughput parallel polymerization reactor (PPR) runs for preparation of polyethylene and ethylene/tBA copolymers.

Polyolefin catalysis screening was performed in a high throughput parallel polymerization reactor (PPR) system. The PPR system was comprised of an array of 48 single cell (6 x 8 matrix) reactors in an inert atmosphere glovebox. Each cell was equipped with a glass insert with an internal working liquid volume of approximately 5 mL. Each cell had independent controls for pressure and was continuously stirred at 800 rpm. Catalysts were prepared in toluene. All liquids (i.e., solvent, tBA, and catalyst solutions) were added via robotic syringes. Gaseous reagents (i.e., ethylene) were added via a gas injection port. Prior to each run, the reactors were heated to 50 °C, purged with ethylene, and vented.

All desired cells were injected with tBA followed with a portion of toluene (This step was skipped for ethylene homopolymerization). The reactors were heated to the run temperature and then pressured to the appropriate psig with ethylene. Catalyst were then added to the cells. Each catalyst addition was chased with a small amount of toluene so that after the final addition, a total reaction volume of 5 mL was reached. Upon addition of the catalyst, the PPR software began monitoring the pressure of each cell. The desired pressure (within approximately 2-6 psig) was maintained by the supplemental addition of ethylene gas by opening the valve at the set point minus 1 psi and closing it when the pressure reached 2 psi higher. The pressure of each cell was monitored during and after the quench to ensure that no further ethylene consumption happens. The shorter the “Quench Time” (the duration between catalyst addition and oxygen quench), the more active the catalyst. All drops in pressure were

cumulatively recorded as “Uptake” or “Conversion” of the ethylene for the duration of the run. After 1h, each reaction was then quenched by addition of 1% oxygen in nitrogen for 30 seconds at 40 psi higher than the reactor pressure. After all the reactors were quenched they were allowed to cool to about 60 °C. They were then vented and the tubes were removed. The polymer samples were then dried in a centrifugal evaporator at 60 °C for 12 hours, weighed to determine polymer yield and submitted for IR (tBA incorporation) and GPC (molecular weight) analysis. NMR analysis were performed separately for microstructural analysis.

5.1.2 General procedure for polymer characterization

a) Gel permeation chromatography (GPC)

High temperature GPC analysis was performed using a Dow Robot Assisted Delivery (RAD) system equipped with a Polymer Char infrared detector (IR5) and Agilent PLgel Mixed A columns. Decane (10 μ L) was added to each sample for use as an internal flow marker. Samples were first diluted in 1,2,4-trichlorobenzene (TCB) stabilized with 300 ppm butylated hydroxyl toluene (BHT) at a concentration of 10 mg/mL and dissolved by stirring at 160°C for 120 minutes. Prior to injection the samples are further diluted with TCB stabilized with BHT to a concentration of 3 mg/mL. Samples (250 μ L) are eluted through one PL-gel 20 μ m (50 x 7.5 mm) guard column followed by two PL-gel 20 μ m (300 x 7.5 mm) Mixed-A columns maintained at 160 °C with TCB stabilized with BHT at a flowrate of 1.0 mL/min. The total run time was 24 minutes. To calibrate for molecular weight (MW) Agilent EasiCal polystyrene standards (PS-1 and PS-2) were diluted with 1.5 mL TCB stabilized with BHT and dissolved by stirring at 160 °C for 15 minutes. These standards are analyzed to create a 3rd order MW calibration curve. Molecular weight units are converted from polystyrene (PS)

to polyethylene (PE) using a daily Q-factor calculated to be around 0.4 using the average of 5 Dowlex 2045 reference samples.

b) Fourier-transform infrared spectroscopy (FTIR)

The 10 mg/mL samples prepared for GPC analysis are also utilized to quantify tert butyl acrylate (tBA) incorporation by Fourier Transform infrared spectroscopy (FTIR). A Dow robotic preparation station heated and stirred the samples at 160°C for 60 minutes then deposited 130 µL portions into stainless wells promoted on a silicon wafer. The TCB was evaporated off at 160°C under nitrogen purge. IR spectra were collected using a Nexus 6700 FT-IR equipped with a DTGS KBr detector from 4000-400 cm⁻¹ utilizing 128 scans with a resolution of 4. Ratio of tBA (C=O: 1762-1704 cm⁻¹) to ethylene (CH₂: 736-709 cm⁻¹) peak areas were calculated and fit to a linear calibration curve to determine total tBA.

c) Differential scanning calorimetry (DSC)

Differential scanning calorimetry analyses was performed on solid polymer samples using a TA Instruments, Inc. Discovery Series or TA Instruments, Inc., DSC2500, programmed with the following method:

Equilibrate at 175.00 °C

Isothermal for 3 minutes

Ramp 30.00 °C/min to 0.00 °C

Ramp 10.00 °C/min to 175.00 °C

Data was analyzed using TA Trios software.

5.2 Original polymerization runs for ethylene/tBA copolymerization in high throughput parallel polymerization reactors (PPR)

Table S5.1. Ethylene copolymerization with **2lut-Me**, **2-CCO** and **2**.

Entry ^a	catalyst	[tBA]/M	Yield (mg)	Act. ^b	M _w /10 ³	PDI	%Mol tBA	Tm (°C)
1	2lut-Me	0.025	75	300	17.7	2.2	0.4	128
2	2lut-Me	0.025	89	356	16.6	2.2	0.4	129
3	2lut-Me	0.025	86	344	15.7	2.2	0.4	128
4	2lut-Me	0.05	40	160	14.8	2.3	0.8	124
5	2lut-Me	0.05	40	160	15.0	2.4	0.8	124
6	2lut-Me	0.05	38	152	16.3	2.5	0.8	124
7	2-CCO	0.025	73	296	18.2	2.2	0.5	127
8	2-CCO	0.025	75	300	18.1	2.4	0.4	128
9	2-CCO	0.025	79	316	17.8	2.4	0.4	128
10	2-CCO	0.05	33	132	17.2	2.4	0.8	125
11	2-CCO	0.05	36	144	17.6	2.5	0.8	124
12	2-CCO	0.05	35	140	17.0	2.7	0.8	124
13 ^c	2	0.05	51	204	16.1	2.3	0.7	121

^aConditions unless specified: catalyst, 0.25 μmol; V(toluene)=5 ml; ethylene pressure=400 psi; T = 70 °C; t = 1h. ^b 1000 kg/(mol·h). ^cData reported in Ref 2.

6. Crystallographic Information

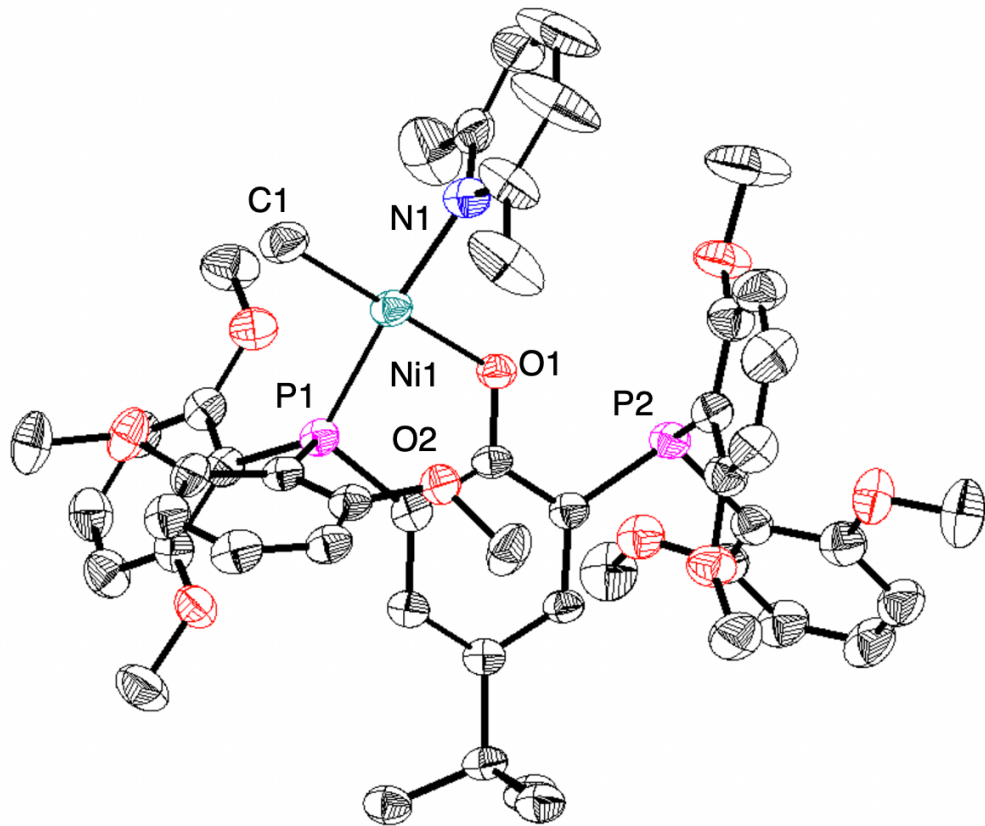


Figure S6.1: Solid-State Structure of **1lut-Me**. Ellipsoids are show at the 50% probability level. Hydrogen atoms excluded for clarity.

Special Refinement Details for **1lut-Me**:

Complex **1lut-Me** crystallizes in the triclinic P-1 space group with cocrystallized toluene in the asymmetric unit. The solvent molecules show relatively broad ellipsoids consistent with a high degree of thermal motion in the solid-state.

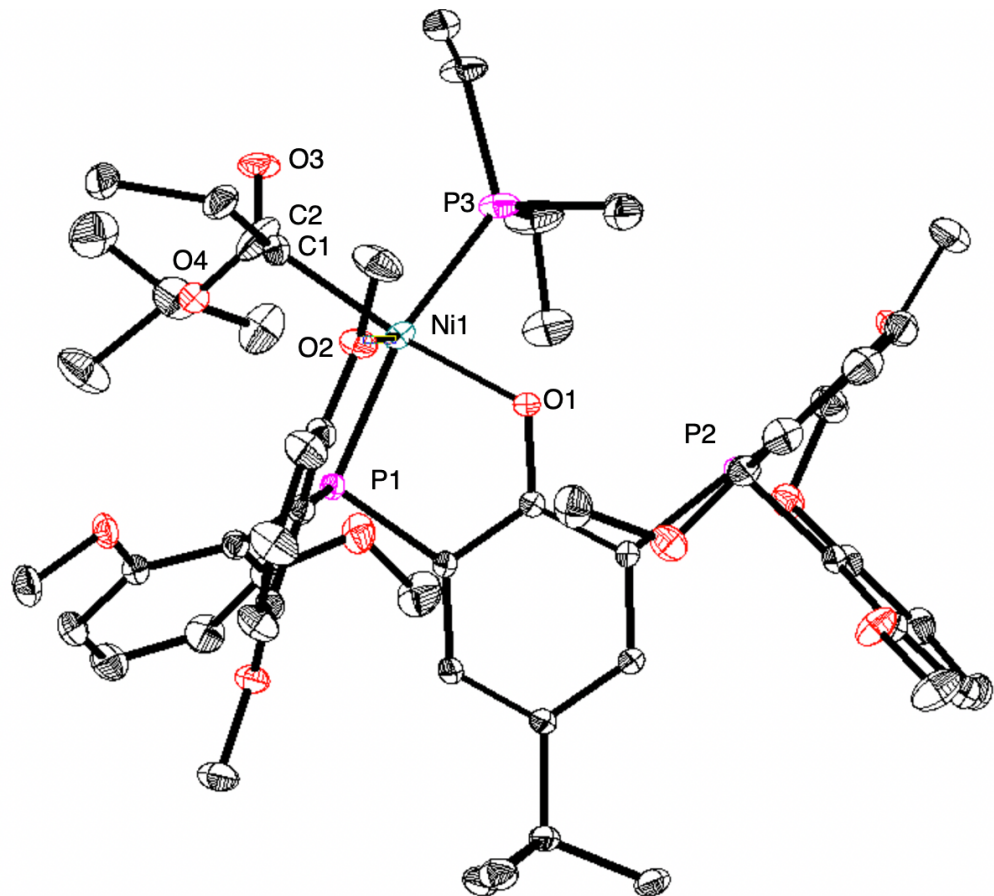


Figure S6.2: Solid-State Structure of **1P-CCO**. Ellipsoids are show at the 50% probability level. Hydrogen atoms excluded for clarity.

Special Refinement Details for **1P-CCO**:

Complex **1P-CCO** crystallizes in the monoclinic $P_{21/n}$ spacegroup. The inserted acrylate moiety suffers from two-site positional disorder and are freely refined to produce relative occupancies of 0.65 and 0.31. The small and plate-like nature of the crystal is responsible for the above average R_{int} value.

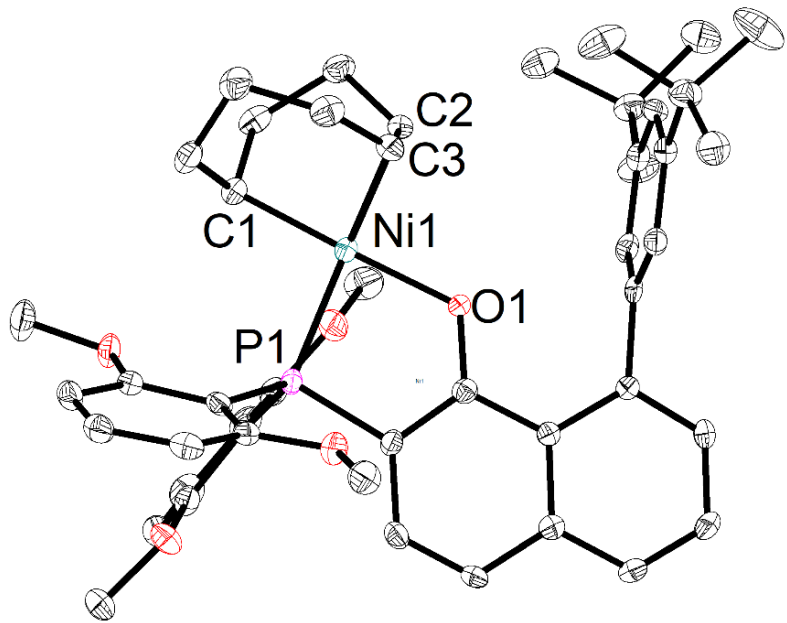


Figure S6.3: Solid-State Structure of $2\text{-C}_8\text{H}_{13}$. Ellipsoids are show at the 50% probability level. Hydrogen atoms excluded for clarity.

Special Refinement Details for $2\text{-C}_8\text{H}_{13}$: Complex $2\text{-C}_8\text{H}_{13}$ crystalizes in a P-1 space group with the full molecule in the asymmetric unit. The SiMe_3 group is modelled with two-site disorder with occupancies of 0.78 and 0.22. One of the methoxy groups is also modelled with two-site disorder with occupancies of 0.78 and 0.22. The carbon on the lower occupancy disordered methoxy group is refined isotropically to prevent a NPD. A disordered benzene molecule is observed and is refined isotropically to prevent NPDs. There is likely disorder on the benzene molecule, despite efforts, it could not be modelled.

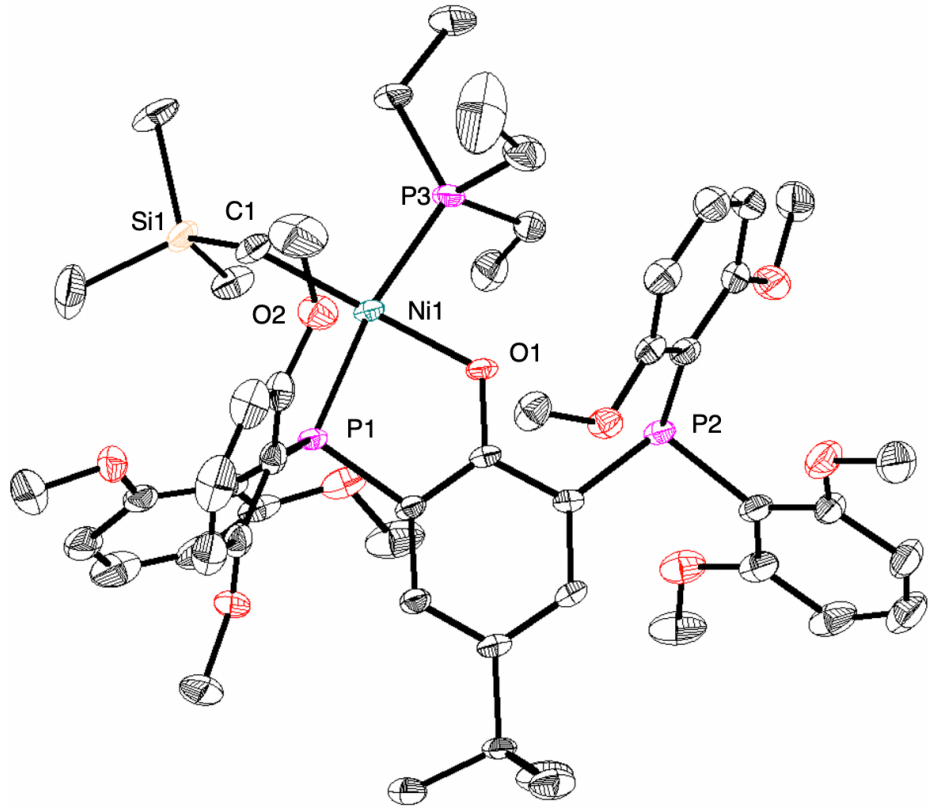


Figure S6.4: Solid-State Structure of **1P**. Ellipsoids are show at the 50% probability level. Hydrogen atoms excluded for clarity.

Special Refinement Details for **1P**:

Complex **1P** crystallizes in the orthorhombic $Pca2_1$ space group with cocrystallized diethyl ether in the asymmetric unit.

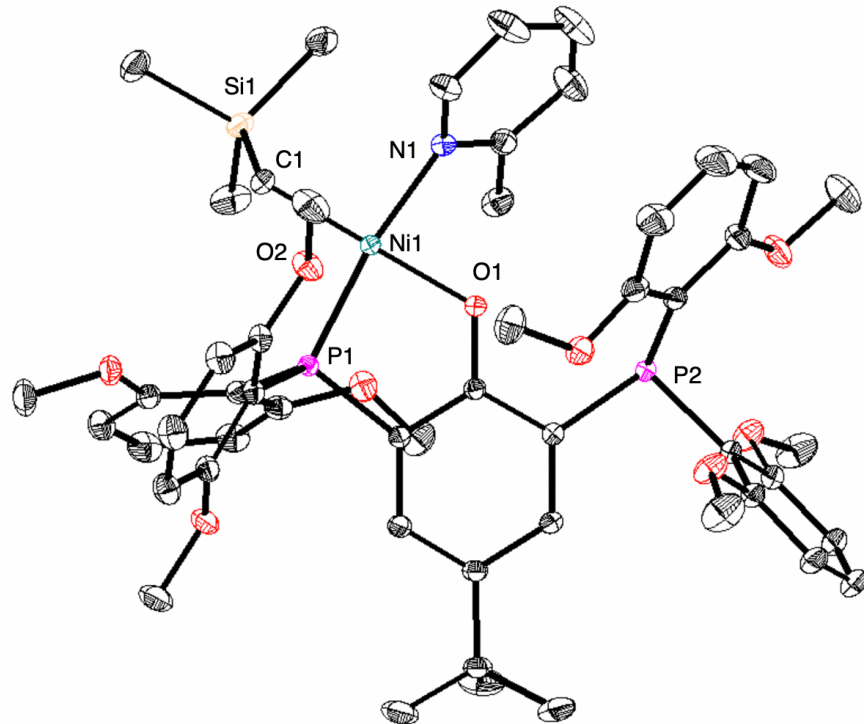


Figure S6.5: Solid-State Structure of **1pico**. Ellipsoids are show at the 50% probability level. Hydrogen atoms excluded for clarity.

Special Refinement Details for **1pico:**

Complex **1pico** crystallizes in the triclinic P-1 space group with a single molecule of benzene cocrystallized in the asymmetric unit along with a half of a benzene molecule.

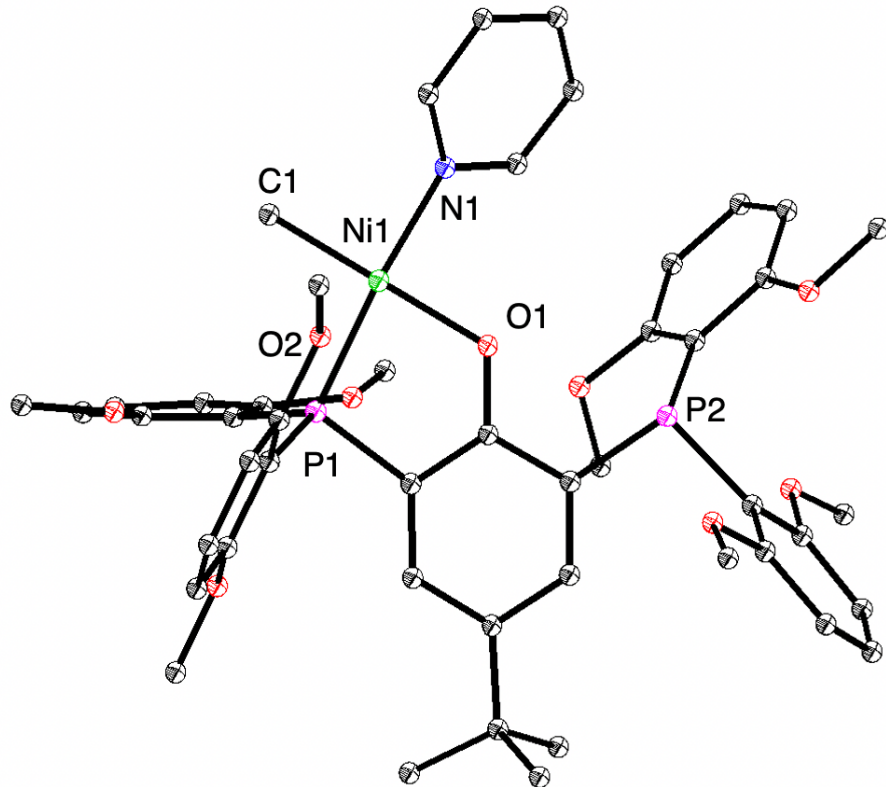


Figure S6.6: Solid-State Structure of **1py-Me**. Ellipsoids are show at the 50% probability level. Hydrogen atoms excluded for clarity.

Special Refinement Details for 1py-Me:

Complex **1py-Me** crystallizes in the triclinic P-1 space group with cocrystallized benzene in the asymmetric unit. The solution suffers from a high R_{int} due to the small size of the single-crystalline sample along with the plate-like shape of the sample

Table S6.1: Crystal and refinement data (part 1)

	2-C₈H₁₃	1P-CCO
CCDC	2173353	2173358
Empirical formula	C ₄₈ H ₅₇ NiO ₅ P	C _{56.42} H _{75.51} NiO _{10.92} P ₃
Formula weight	803.61	1080.16
Temperature/K	100	100
Crystal system	Monoclinic	Monoclinic
Space group	C _{2/c}	P21/n
a/Å	41.799(11)	14.637(3)
b/Å	12.951(2)	16.793(4)
c/Å	15.734(5)	22.546(5)
α/°	90	90
β/°	105.463(16)	94.948(14)
γ/°	90	90
Volume/Å ³	8209(4)	5521(2)
Z	8	4
ρ _{calc} g/cm ³	0.066	0.496
μ/mm ⁻¹	1.414	1.300
F(000)	3424	2298
Radiation	CuKα	MoKα
Reflections collected	7891	200549
Independent reflections	6893	9989
Goodness-of-fit on F ²	1.064	0.940
R _{int}	twinned	27.81%

Table S6.2: Crystal and refinement data (part 2)

	1lut-Me	1py-Me
CCDC	2173356	2173354
Empirical formula	C ₅₇ H ₆₇ NNiO ₉ P ₂	C ₅₄ H ₆₁ NNiO ₉ P ₂
Formula weight	1030.76	988.68
Temperature/K	100	100
Crystal system	Triclinic	Triclinic
Space group	P-1	P-1
a/Å	12.408(2)	13.3937(14)
b/Å	14.666(6)	13.8200(15)
c/Å	15.040(4)	13.8909(14)
α/°	93.413(18)	79.649(6)
β/°	96.340(13)	76.070(10)
γ/°	96.33(2)	87.758(7)
Volume/Å ³	2965.5(14)	2454.9(5)
Z	2	2
ρ _{calc} g/cm ³	1.270	1.338
μ/mm ⁻¹	1.528	1.656
F(000)	1092	1044
Radiation	CuKα	CuKα
Reflections collected	32411	116262
Independent reflections	6900	9583
Goodness-of-fit on F ²	1.071	1.076
R _{int}	8.60%	34.92%

Table S6.3: Crystal and refinement data (part 3)

	1P	1pico
CCDC	2173355	2173352
Empirical formula	C ₅₆ H ₈₃ NiO ₁₀ P ₃ Si	C ₆₇ H ₈₀ NNiO ₉ P ₂ Si
Formula weight	1095.93	1192.06
Temperature/K	100	100
Crystal system	Orthorhombic	Triclinic
Space group	P-2ac	P-1
a/Å	26.600(9)	13.037(5)
b/Å	14.884(4)	13.920(3)
c/Å	14.618(3)	19.809(6)
α/°	90	96.29(3)
β/°	90	105.302(19)
γ/°	90	111.175(12)
Volume/Å ³	5788(3)	3148.3(18)
Z	4	2
ρ _{calc} g/cm ³	1.258	1.257
μ/mm ⁻¹	0.493	0.434
F(000)	2344	1266
Radiation	MoKα	MoKα
Reflections collected	117397	257499
Independent reflections	9541	9470
Goodness-of-fit on F ²	0.848	1.058
Final R indexes [I>=2σ (I)]	7.33%	5.74

7. Computational Details

DFT energy calculations and geometry optimizations in the gas phase are carried out with Gaussian software.⁵ The hybrid meta-generalized gradient approximation (hybrid meta-GGA) functional M06⁶ was used with the Karlsruhe-family double- ζ valence basis set def2-SVP.⁷ M06 was chosen for its extensive benchmarking with organometallic systems⁸ and from prior use in related systems.² When available, the initial guess for geometry optimization was the experimental X-ray crystal structure. Conformational sampling was performed using Entos Qcore software⁹ by running an annealing MD trajectory for a given structure using the GFN-xTB1¹⁰ potential energy surface, followed by optimization at the XTB level, and finally DFT optimization using the M06 functional. The critical points on the potential energy surface are confirmed with harmonic frequency analysis, where exactly zero imaginary frequencies are seen for ground-state structures. Single point corrections are performed using the M06 functional and the triple- ζ def2-TZVP basis set. Implicit solvation effects by toluene solvent are considered by using the SMD continuum solvation model¹¹ as an additional single point correction with the ORCA software package.¹³ Gibbs free energies are taken at 298.15 K. Natural charges at the nickel metal center were taken using natural bond orbital (NBO) analysis.¹³

In Figure 10, the following ligands bound to the Ni center were considered for each catalyst **2L** ($R =$ silane), **2L-Me** ($R =$ Me), and **2L-CCO** ($R =$ ester): pyridine, 1,5-dimethylpyridine, 5-fluoropyridine, ethene, butene, hexene, methyl vinyl ether (binding at alkene), methyl vinyl ether (binding at O), vinyl acetate (binding at alkene), vinyl acetate (binding at O), *t*-butyl acrylate (binding at alkene), *t*-butyl acrylate (binding at O),

acrylonitrile (binding at alkene), acrylonitrile (binding at N), methyl vinyl ketone (binding at alkene), and methyl vinyl ketone (binding at O).

Regression analysis was performed on the data in Figure 10. The lines of regression for the catalyst systems **2L** ($R = \text{silane}$) and **2L-Me** ($R = \text{Me}$) are $y = 0.98x + 3.07 \text{ kcal/mol}$ ($R^2 = 0.82$) and $y = 1.00x + 2.25 \text{ kcal/mol}$ ($R^2 = 0.79$), respectively.

8. Reference

- 1) Pangborn, A. B.; Giardello, M. A.; Grubbs, R. H.; Rosen, R. K.; Timmers, F. J. Safe and convenient procedure for solvent purification. *Organometallics* **1996**, *15*, 1518-1520
- 2) Shuoyan Xiong, Manar M. Shoshani, Xinglong Zhang, Heather A. Spinney, Alex J. Nett, Briana S. Henderson, Thomas F. Miller III, Theodor Agapie. "Efficient Copolymerization of Acrylate and Ethylene with Neutral P, O-Chelated Nickel Catalysts: Mechanistic Investigations of Monomer Insertion and Chelate Formation" *J. Am. Chem. Soc.* **2021**, *143*, 6516-6527
- 3) Connor, E. F.; Younkin, T. R.; Henderson, J. I.; Waltman, A. W.; Grubbs, R. H. Synthesis of neutral nickel catalysts for ethylene polymerization—the influence of ligand size on catalyst stability. *Chem. Commun.* **2003**, 2272-2273.
- 4) Palmer, W. N.; Zarate, C.; Chirik, P. J. Benzyltriboroborates: Building Blocks for Diastereoselective Carbon–Carbon Bond Formation. *J. Am. Chem. Soc.* **2017**, *139*, 2589-2592.
- 5) Frisch, M. J.; Trucks, G. W.; Schlegel, H. B.; Scuseria, G. E.; Robb, M. A.; Cheeseman, J. R.; Scalmani, G.; Barone, V.; Mennucci, B.; Petersson, G. A.; et al. Gaussian 16, Revision A.01. 2016.
- 6) Zhao, Y.; Truhlar, D. G. The M06 Suite of Density Functionals for Main Group Thermochemistry, Thermochemical Kinetics, Noncovalent Interactions, Excited States, and Transition Elements: Two New Functionals and Systematic Testing of Four M06-Class Functionals and 12 Other Function. *Theor. Chem. Acc.* **2008**, *120* (1), 215–241.
- 7) Weigend, F.; Ahlrichs, R. Balanced Basis Sets of Split Valence, Triple Zeta Valence and Quadruple Zeta Valence Quality for H to Rn: Design and Assessment of Accuracy. *Phys. Chem. Chem. Phys.* **2005**, *7* (18), 3297–3305.
- 8) Yu, H. S.; He, X.; Li, S. L.; Truhlar, D. G. MN15: A Kohn–Sham Global-Hybrid Exchange–Correlation Density Functional with Broad Accuracy for Multi-Reference and Single-Reference Systems and Noncovalent Interactions. *Chem. Sci.* **2016**, *7* (8), 5032–5051.
- 9) Manby, F. R.; Miller, T. F.; Bygrave, P. J.; Ding, F.; Dresselhaus, T.; Buccheri, A.; Bungey, C.; Lee, S. J. R.; Meli, R.; Steinmann, C.; et al. Entos : A Quantum Molecular Simulation Package. *ChemRxiv*. **2019**.
- 10) Grimme, S.; Bannwarth, C.; Shushkov, P. A Robust and Accurate Tight-Binding Quantum Chemical Method for Structures, Vibrational Frequencies, and Noncovalent Interactions of Large Molecular Systems Parametrized for All Spd-Block Elements ($Z = 1\text{--}86$). *J. Chem. Theory Comput.* **2017**, *13* (5), 1989–2009.
- 11) Marenich, A. V.; Cramer, C. J.; Truhlar, D. G. Universal Solvation Model Based on Solute Electron Density and on a Continuum Model of the Solvent Defined by the Bulk Dielectric Constant and Atomic Surface Tensions. *J. Phys. Chem. B* **2009**, *113* (18), 6378–6396.

12) Neese, F.; Wennmohs, F.; Becker, U.; Riplinger, C. The ORCA quantum chemistry program package. *J. Chem. Phys.* **2020**, *152*, 224108.

13) Reed, A. E.; Weinstock, R. B.; Weinhold, F. J. Natural population analysis. *Chem. Phys.* **1985**, *83*, 735-746.